

## Trends in atmospheric new-particle formation: 16 years of observations in a boreal-forest environment

Tuomo Nieminen<sup>1),2)</sup>, Ari Asmi<sup>1)</sup>, Miikka Dal Maso<sup>3)</sup>, Pasi P. Aalto<sup>1)</sup>,  
Petri Keronen<sup>1)</sup>, Tuukka Petäjä<sup>1)</sup>, Markku Kulmala<sup>1)</sup> and Veli-Matti Kerminen<sup>1)</sup>

<sup>1)</sup> Department of Physics, P.O. Box 64, FI-00014 University of Helsinki, Finland

<sup>2)</sup> Helsinki Institute of Physics, P.O. Box 64, FI-00014 University of Helsinki, Finland

<sup>3)</sup> Department of Physics, Tampere University of Technology, P.O. Box 692, FI-33101 Tampere, Finland

Received 17 Dec. 2013, final version received 17 Mar. 2014, accepted 28 Mar. 2014

Nieminen, T., Asmi, A., Dal Maso, M., P. Aalto, P., Keronen, P., Petäjä, T., Kulmala, M. & Kerminen, V.-M. 2014: Trends in atmospheric new-particle formation: 16 years of observations in a boreal-forest environment. *Boreal Env. Res.* 19 (suppl. B): 191–214.

New-particle formation (NPF) is globally an important source of climatically-relevant atmospheric aerosols. Here we explore the inter-annual variability and trends in sources and sinks of atmospheric nanoparticles in a boreal forest environment. We look into the precursor vapors leading to the aerosol formation, NPF frequency, as well as the formation and growth rates of the freshly-formed particles. The analysis is based on 16 years of data acquired from the Station for Measuring Ecosystem–Atmosphere Relations (SMEAR II) in Hyytiälä, Finland. The results indicate that the probability of NPF is connected to both air mass origin, explaining a large part of the year-to-year variability in the number of NPF events, and concentrations of low-volatile vapours. The probability of NPF increases with increasing gaseous sulphuric acid concentrations, but even better association is found between the NPF probability and product of sulphuric acid and low-volatile organic vapour (proxy) concentrations. While the concentrations of both sulphuric acid (evaluated by proxy) and sulphuric-acid precursor sulphur dioxide decreased over the 16-year measurement period, the new-particle formation and growth rates slightly increased. On the other hand, the proxy concentrations of oxidized organics increased in all seasons except in winter. The contribution of sulphuric acid to the particle growth was minor, and the growth rate had a clear connection with the ambient temperature due to higher emissions of biogenic volatile organic compounds at higher temperatures. For a given sulphuric acid concentration evaluated by proxy, particle formation rates tended to be higher at higher temperatures.

### Introduction

Research on new-particle formation (NPF) in the atmosphere has been very active during the last two decades. This phenomenon has been

observed in various environments around the world [*see Kulmala et al. (2004) for a comprehensive review of observations, and also Kulmala and Kerminen 2008*], including clean and polluted continental areas (Birmili *et al.* 2003),

ocean coastal areas (O'Dowd *et al.* 2002), pollution plumes, outflows from convective clouds and free troposphere (Krejci *et al.* 2003).

Based on field measurements, theoretical considerations and laboratory experiments, the key compound that has been found to participate in the atmospheric NPF is sulphuric acid (Kerminen *et al.* 2010, Sipilä *et al.* 2010, Petäjä *et al.* 2011). The intensity of the NPF, described by the particle formation rate, has generally been found to vary to the power of 1–2 of the sulphuric acid concentration (Weber *et al.* 1995, Kulmala *et al.* 2006, Nieminen *et al.* 2009, Paasonen *et al.* 2010). Other vapors that are potentially important for the atmospheric NPF include ammonia (e.g. Korhonen *et al.* 1999, Kulmala *et al.* 2003, Weber *et al.* 2003), amines which could enhance the sulphuric acid–water nucleation even more than ammonia (*see e.g.* Kurtén *et al.* 2008, Loukonen *et al.* 2010, Kirkby *et al.* 2011, Zhao *et al.* 2011, Yu *et al.* 2012, Almeida *et al.* 2013), low-volatile biogenic vapours and their oxidation products (Kulmala *et al.* 1998, Metzger *et al.* 2010), and in coastal areas also iodine oxides (O'Dowd *et al.* 2002, Yoon *et al.* 2006, Ehn *et al.* 2010). Gaseous sulphuric acid ( $\text{H}_2\text{SO}_4$ ) present in the atmosphere is produced mainly via the oxidation of sulphur dioxide ( $\text{SO}_2$ ) by the OH radical. The OH radical is formed by the photolysis of ozone, thus requiring sunlight for its production. As a result, the strongest and long-lasting events of the atmospheric NPF are typically observed during the daytime when also atmospheric photo-chemistry is most intense (Kulmala and Kerminen 2008), even though there are also observations of the nighttime NPF events (e.g. Junninen *et al.* 2008, Kalivitis *et al.* 2012).

Atmospheric aerosol particles affect the Earth's climate system via aerosol–radiation and aerosol–cloud interactions (IPCC 2013), and the latter effect depends strongly on the sub-population of aerosol particles able to act as cloud condensation nuclei (CCN). The atmospheric NPF has been shown to enhance CCN concentrations regionally (Laaksonen *et al.* 2005, Wiedensohler *et al.* 2009, Sihto *et al.* 2011, Laakso *et al.* 2013, Paramonov *et al.* 2013), and the enhancement is very likely to be globally important as well (Spracklen *et al.* 2008, Merikanto *et al.* 2009, Yu and Luo 2009, Kerminen *et al.* 2012). The

atmospheric CCN budget depends, however, in a complicated way on both primary and nucleated aerosol particles and their interactions (Alm *et al.* 2013, Lee *et al.* 2013), causing substantial uncertainties in the current and future climatic forcing and associated feedbacks (Kazil *et al.* 2010, Makkonen *et al.* 2012, Ghan *et al.* 2013, Paasonen *et al.* 2013, Spracklen and Rap 2013).

Efforts to control air pollution since the 1970s have decreased the emissions of many gaseous pollutants such as sulphur dioxide ( $\text{SO}_2$ ), nitrogen oxides ( $\text{NO}_x$ ) and carbon monoxide (CO), as well as concentrations of submicron ( $\text{PM}_{10}$ ), fine ( $\text{PM}_{2.5}$ ) and respirable ( $\text{PM}_{10}$ ) particulate matter in Europe (The Emissions Database for Global Atmospheric Research, 2011, EC-JRC/PBL, EDGAR ver. 4.2, <http://edgar.jrc.ec.europa.eu/>). In many areas of Finland, the concentration levels of air pollutants have been low already in the past compared with many other regions of Europe, yet these concentrations have been found to decrease also in Finland during the last decades (Anttila *et al.* 2010). Long-range transport from central and eastern Europe in air masses coming from the south and south-east influences also the pollutant levels in Finland (Riuttanen *et al.* 2013). During the last decade the overall trend in many aerosol properties in northern Europe, specifically the submicron particle number concentration (both in total and in the size ranges larger than 100 nm diameter, Asmi *et al.* 2013) and aerosol scattering Ångström exponent (Collaud Coen *et al.* 2013), was decreasing.

In this paper, we investigate long-term changes in atmospheric new-particle formation and growth at the University of Helsinki research station in Hyytiälä, southern Finland. The first analyses of the atmospheric NPF events at this station were reported by Mäkelä *et al.* (1997) and Kulmala *et al.* (1998). Dal Maso *et al.* (2005) published the first results of the annual and seasonal patterns in new-particle formation at this site, whereas particle growth rates and their seasonal variation at the site were investigated by Hirsikko *et al.* (2005) and Yli-Juuti *et al.* (2011). The main focus of this paper is on the role of  $\text{SO}_2$  and pre-existing particle concentrations on the temporal variation and long-term trends in the NPF in Hyytiälä, as these two quantities together with solar radiation intensity

determine the gas-phase sulphuric acid concentration. Since there are no continuous long-term measurements of sulphuric acid concentrations in Hyytiälä, we calculated proxy concentrations based on a simple steady-state balance equation (Petäjä *et al.* 2009). Trends in the frequency of new-particle formation are investigated based on the yearly number of NPF event days, as well as the magnitude of particle formation and growth rates and their correlations with other parameters, such as sulphuric acid evaluated by proxy, temperature and air-mass arrival directions. The specific questions we aim to answer are: (1) Did the NPF frequency, magnitude and seasonal variability change with time? (2) What are the factors influencing the frequency of the NPF? (3) What is the connection between sulphuric acid and new-particle formation and growth rates? (4) What is the role of organic compounds? (5) Are there indications of long-term trends in the NPF and what are the key factors influencing this quantity?

## Material and methods

### Measurements

In this study, we utilized the data from the University of Helsinki SMEAR II station measurement network. The station is equipped with extensive facilities to measure continuously and comprehensively interactions between the atmosphere and the forest ecosystem. A detailed description of the continuous measurements conducted at this station can be found in Kulmala *et al.* (2001) and Hari and Kulmala (2005). Here we give an overview of those measurements that were used in analyzing the long-term trends in particle formation.

The SMEAR II station is located in southern Finland (61°51'N, 24°17'E, 181 m a.s.l.) 220 km SW from Helsinki. The nearest large city (200 000 inhabitants) is Tampere located about 60 km SW from the station. Considering the levels of air pollutants, shown by e.g. submicron aerosol number size distributions (Asmi *et al.* 2011b), Hyytiälä is a rural, background site. The station is surrounded by rather homogeneous Scots-pine-dominated forests.

The core instrumentation operated since January 1996 includes a 74-m-high mast (extended to 126 m in summer 2010) and aerosol number concentration and size distribution measurement systems. From the mast, concentrations of trace gases SO<sub>2</sub>, NO, NO<sub>x</sub>, O<sub>3</sub>, CO and CO<sub>2</sub> are measured at 6 heights. In this study, we used the SO<sub>2</sub> measurements made using a UV-fluorescence analyser (trace level model series 43, Thermo Fisher Scientific, Waltham, MA, USA) that has a detection limit of 0.1 ppb. In order to minimize any possible effects of local pollution sources, we used SO<sub>2</sub> from the highest level (67 m above ground). There were no large differences in the overall SO<sub>2</sub>, NO, NO<sub>x</sub> and CO concentration levels among the different measurement heights. Solar radiation in the UV-B wavelengths (280–320 nm) and global radiation (0.3–4.8 μm) were measured with pyranometers (SL 501A UVB, Solar Light, Philadelphia, PA, USA; Reemann TP 3, Astrodata, Tõravere, Tartumaa, Estonia, until June 2008, and Middleton Solar SK08, Middleton Solar, Yarraville, Australia, since June 2008). The data from these measurements were arithmetically averaged to a 30-min time resolution. Aerosol particle number concentration size distributions were measured with a twin-DMPS system (Aalto *et al.* 2001). The system consists of two separate DMPS instruments, one measuring particles between 3 and 50 nm and the other larger particles. The collective size range of the twin-DMPS system was from 3 to 500 nm until December 2004, and after that it was extended to cover the size range from 3 nm to 1000 nm. In September 2004, the DMPS system was moved to a new, similar measurement location about 200 m from the original one.

Air-mass arrival directions and source areas were investigated using 96-hour back-trajectories calculated using HYSPLIT\_4, a Lagrangian transport model developed by NOAA and freely available on the internet (<http://www.arl.noaa.gov/HYSPLIT.php>). Input meteorological data for the model were taken from the GDAS (Global Data Assimilation System) archives. Trajectories were calculated for a 100-m arrival height once per hour. We examined air mass arrival directions in two sectors, from northwest-to-north (280°–30°), and outside this sector, based on the requirement that the air mass had

spent at least 80% of the last 30 hours before arrival in the given sector.

As our study period we used 1 Mar. 1997–28 Feb. 2013, which is when the data coverage from all the instruments was the best for our purposes. The general character of the NPF in Hyytiälä is presented for the years 1996–2012, as the aerosol number size distribution data were available already from 1996 onwards. Many of the parameters investigated here have a strong seasonal variation, and therefore we divided the year into seasons: spring (March–May), summer (June–August), autumn (September–November) and winter (December–February).

## Data analysis

### New-particle formation events

The aerosol number size distribution data were used to classify days according to whether new-particle formation was observed during the day or not. Typically, particle formation starts in Hyytiälä in a time window of a few hours around noon, and is only rarely observed at nighttime, although nanoparticles below 3 nm have been frequently observed in Hyytiälä (Lehtipalo *et al.* 2011). For this reason it is practical to classify the NPF event occurrence on a daily basis.

The guidelines for particle size distribution analysis with respect to the NPF were those originally presented by Dal Maso *et al.* (2005), and most recently by Kulmala *et al.* (2012). Namely, we were looking for signs of regional-scale new-particle formation in distinction from local sources of nanoparticles, such as traffic or emissions from industry. Therefore, two criteria must be met in order for a day to be classified as a NPF event day: there must be a new mode of particles appearing during the day to sizes smaller than 25 nm in mobility diameter, and this new mode must be growing. This imposes more strict conditions for the homogeneity of the air masses during the day, as we need to be able to follow the growth of the nucleation mode particles. This is not always possible if air masses are changing too abruptly during the day. Also this approach to event classification does not take into account new-particle formation that takes

place in a geographically-limited area, where the growth of the particles cannot be followed during the day. Furthermore, from only the clearest NPF events the formation and growth rate of the particles can be reliably determined, and this is why the NPF events are divided into class I (in which the formation and growth rates can be calculated) and class II (clear NPF events, but formation and growth rates cannot be reliably calculated). Days when no new-particles smaller than 25 nm are observed are classified as non-event days. Undefined days are those days for which we are unable to determine unambiguously whether the NPF occurred during the day or not. The NPF event classification was done in groups of 2–3 researchers in order to reduce the subjectivity of the procedure. Not all the data were analysed by the same researchers, yet we are confident that the classification guidelines were robust enough so that this does not bias the results.

### Particle formation and growth rates

The formation rate of nucleation mode particles was determined from the particle number size distributions measured by the DMPS. The number concentration of nucleation-mode particles,  $N_{3-25}$ , of the diameter in the size range 3–25 nm was integrated from the measured number concentration size distributions. Taking into account all the production and loss terms we can write the following balance equation for  $N_{3-25}$ :

$$\frac{dN_{3-25}}{dt} = J_3 - F_{\text{coag}} - F_{\text{growth}}, \quad (1)$$

where  $J_3$  is the observed formation rate of nucleation mode particles larger than 3 nm in diameter, and the loss terms are coagulation with larger particles ( $F_{\text{coag}}$ ) and condensational growth out of nucleation mode ( $F_{\text{growth}}$ ). By rearranging the terms in Eq. 1 and expressing coagulation flux in terms of coagulation sink and condensational growth flux by the observed particle growth rate we get an expression for the formation rate of nucleation mode particles as (Kulmala *et al.* 2012):

$$J_3 = \frac{dN_{3-25}}{dt} + \text{CoagS} \times N_{3-25} + \frac{\text{GR}}{\Delta d_p} N_{3-25}, \quad (2)$$

where GR is the growth rate of nucleation mode particles, CoagS is the coagulation sink that we calculated from the particle number size distributions according to Kulmala *et al.* (2012), and the particle size range,  $\Delta d_p$ , was 3–25 nm, allowing us to calculate and average formation rate for the whole nucleation mode.

The value of GR was obtained by fitting log-normal functions to measured particle number size distributions using the algorithm presented by Hussein *et al.* (2005). This algorithm fits a maximum of three log-normal modes into each individual particle number size distribution. From the fitted particle number size distributions, we selected the growing nucleation mode geometric mean diameters by visual inspection of the size distributions, and the growth rate was calculated as a linear least-squares fit into the data set of the selected nucleation mode geometric mean diameters as function of time (Kulmala *et al.* 2012). This mode-fitting method determines one value of GR for each new-particle formation event, and thus implicitly assumes that the growth rate is constant in the nucleation mode during the particle growth.

The fraction of the observed particle growth rates explained by vapour condensation can be estimated by calculating the particle condensation growth rates based on kinetic gas theory, and by comparing this to the observed particle growth. The growth rate due to condensation of vapour with gas-phase concentration  $C_v$  is given (Nieminen *et al.* 2010) by

$$\text{GR} = \frac{1}{2\rho_v} \left( \frac{8kTm_v}{\pi} \right)^{1/2} \left( 1 + \frac{d_v}{d_p} \right)^2 \left( 1 + \frac{m_v}{m_p} \right)^{1/2} C_v, \quad (3)$$

where  $d_p$  and  $m_p$  are the diameter and mass of the growing particle, respectively, and  $d_v$ ,  $m_v$  and  $\rho_v$  are the diameter, mass and density of the molecules of the condensing vapour, respectively. The condensing vapour was assumed to have molecular properties of sulphuric acid, namely  $d_v = 0.68$  nm,  $m_v = 98$  amu and  $\rho_v = 1.83$  g cm<sup>-3</sup>, and it was assumed to have a negligible saturation vapour pressure.

### Sulphuric acid evaluated by proxy

The proxy for atmospheric sulphuric acid H<sub>2</sub>SO<sub>4</sub>

concentration can be derived from its source and sink terms. H<sub>2</sub>SO<sub>4</sub> is mainly produced in the atmosphere through oxidation of SO<sub>2</sub> by the hydroxyl radical, OH. The hydroxyl radical is formed in the atmosphere when solar radiation breaks ozone molecules forming excited-state oxygen atoms which then react with water molecules. Rohrer and Berresheim (2006) showed that the OH concentration in the lower troposphere strongly correlates with the solar radiation intensity, especially with the UV-B part of the solar spectrum (wavelengths 280–320 nm). Thus, in this work we approximated atmospheric OH concentrations by suitably scaling the UV-B radiation (UVB) and ignoring other sink terms of the OH radicals. The main sink term for H<sub>2</sub>SO<sub>4</sub> is condensation onto pre-existing particle surfaces, which can be described using the condensation sink (CS) calculated from the particle number size distributions according to Kulmala *et al.* (2012). The equation for the steady-state H<sub>2</sub>SO<sub>4</sub> concentration evaluated by proxy is

$$[\text{H}_2\text{SO}_4]_{\text{proxy}} = k \times \frac{[\text{SO}_2] \times \text{UVB}}{\text{CS}}. \quad (4)$$

The scaling coefficient  $k$  is obtained from the comparison of the proxy concentrations to available measured H<sub>2</sub>SO<sub>4</sub> concentration data. In Hyytiälä, H<sub>2</sub>SO<sub>4</sub> has been measured mainly during spring and summer in the years 2003, 2005, 2007, 2010 and 2011. Here we used the value of  $k = 8.4 \times 10^{-7} \times \text{UVB}^{-0.68}$  (m<sup>2</sup> W<sup>-1</sup> s<sup>-1</sup>) based on the 2007 data set presented by Petäjä *et al.* (2009).

More recently, Mikkonen *et al.* (2011) introduced a non-linear proxy in which the production and loss terms of Eq. 4 are allowed to have powers differing from unity. Compared with the linear proxy of Eq. 4, the approach by Mikkonen *et al.* (2011) gives slightly better agreement with the measurement results in some measurement-campaign data sets from Hyytiälä. Since the sulphuric acid measurements in Hyytiälä have been performed only during spring and summer, there are no constraints on the seasonal cycle of measured sulphuric acid concentrations. Hence, it cannot be reliably assessed which of the sulphuric acid proxies gives better agreement with the measurements, and therefore we chose to present here the  $[\text{H}_2\text{SO}_4]_{\text{proxy}}$  results using the approach of Petäjä *et al.* (2009). Petäjä *et al.*



(2009) found that 80% of the proxy concentrations were within a factor of two of the measured concentrations.

Other possible formation mechanisms for sulphuric acid in the atmosphere have also been suggested, both theoretically and based on comparisons between measured and modelled sulphuric acid concentrations (e.g. Mauldin *et al.* 2012, Boy *et al.* 2013). These studies suggest that other oxidation mechanisms can contribute significantly to ambient sulphuric acid concentrations (tens of percents in the lowest 100 m of the boundary layer) during spring. However, in the proxy calculations we decided to examine only the contribution of SO<sub>2</sub> oxidation due to uncertainties related to quantifying the other production mechanisms from the long-term data sets.

### Oxidized organic compounds evaluated by proxy

The measured concentrations of different VOC species have been parametrized as functions of temperature by Lappalainen *et al.* (2009). The parameterization is based on measurements of VOC concentrations in Hyytiälä in June 2006–August 2007. The concentrations of the monoterpene oxidation products by OH and ozone evaluated by proxy, [OxOrg]<sub>proxy</sub>, can be calculated as

$$[\text{OxOrg}]_{\text{proxy}} = \frac{a \exp(bT) (k_{\text{OH}} [\text{OH}]_{\text{proxy}} + k_{\text{O}_3} [\text{O}_3])}{\text{CS}}, \quad (5)$$

where  $T$  (°C) is the ambient temperature, the coefficients  $a = 0.062$  ppb and  $b = 0.078$  °C<sup>-1</sup> are taken from the parameterization by Lappalainen *et al.* (2009), and the coefficients  $k_{\text{OH}} = 7.5 \times 10^{-11}$  cm<sup>3</sup> s<sup>-1</sup> and  $k_{\text{O}_3} = 1.4 \times 10^{-17}$  cm<sup>3</sup> s<sup>-1</sup> are the averages of the reaction rate coefficients for individual monoterpene species weighted according to their typical concentrations found in Hyytiälä. The OH concentration was approximated by scaling the measured UV-B radiation similarly as in the case of [H<sub>2</sub>SO<sub>4</sub>]<sub>proxy</sub>

$$[\text{OH}]_{\text{proxy}} = \left( \frac{8.4 \times 10^{-7}}{8.6 \times 10^{-10}} \text{UVB}^{0.32} \right)^{1.92}. \quad (6)$$

### Trend estimation

Several methods have been used to estimate rates of change of environmental variables. One issue to determine when analysing trends in time-series data sets is whether the trend is linear in time, or whether it has more complicated time behaviour. For example, the magnitude of the trend can change over time from decreasing to increasing or vice versa. Another issue is related to determining the magnitude and statistical significance of the trend; see Weatherhead *et al.* (1998) and Hess *et al.* (2001) for review of the methods of the trend estimation from environmental data series.

In this study, we chose to treat all the trends as linear functions of time in order to keep the approach as simple as possible. The fitting was done to logarithmic values of the data, since most atmospheric quantities (such as trace gas and aerosol particle number concentrations) are close to log-normally distributed. In this respect, the studied trends are thus relative changes in the absolute concentrations. Hence, we fitted a model

$$\log_{10} y = at + b \quad (7)$$

to the data points of measurements of the variable  $y$  as function of time  $t$ . The fitting of Eq. 7 was done using the Matlab *robustfit* algorithm, which is an iteratively reweighted least squares method with a bisquare weighting function (Street *et al.* 1988). Notably, minimizing is then done on the relative distance of the concentrations to the fitting line. The slope  $a$  obtained from the fit to logarithmic data tells directly the rate of change of the quantity  $y$  in percentages per unit of time. Only in the case of calculating the trend for UV-B radiation, we fitted the actual data values, not their logarithms.

When determining the existence of a statistically significant trend in the data set we used a variation of a bootstrap method called moving-block bootstrapping (MBB; for details see Mudelsee 2000). This method is similar to the monthly-data trend fitting done by Asmi *et al.* (2013). In this method, new time-series of the data are constructed by randomly selecting blocks of residuals from the original trend fitting.

The block size used was one year, starting from the 1st of January. The trend model (Eq. 7) was then fitted to this resampled time series, and the slope of the new fit was stored. After repeating the bootstrapping process for 1000 times, we obtained a distribution of the fitted slope values and selected the 5th and 95th percentiles to represent the confidence interval of the fitted slope (Table 1). This confidence interval thus gave an estimate of the effect of the inter-annual variation around the trend line to the overall trend slopes, without the need for specifically complicating the trend model with seasonal or autocorrelation terms. If the 5th and 95th percentiles had the same sign we regarded the trend as statistically significant.

## Results and discussion

### Annual cycle of NPF frequency in Hyytiälä

The analysis of the general characteristics of the NPF in Hyytiälä presented in this section extends those published by Dal Maso *et al.* (2005, 2007) by doubling the length of the examined data set. During the years 1996–2012, the total number of NPF event days was 1418. Annually, the number of event days varied in the range 60–120. The highest number of NPF events was observed in the years 2002–2004 when during each year more than 110 days were categorized as event days. The NPF events were least frequent in 1998 and 2010 with less than 70 NPF event days in both years. The average yearly fraction of NPF event days was 23%, which is comparable to the fraction reported by Dal Maso *et al.* (2007).

The seasonal distribution of the NPF events differed to some extent from year to year, even though spring was the most frequent event time in all the years (Fig. 1). Typically, the NPF occurred more frequently in autumn than in summer, but in some years there were more NPF event days in summer than in autumn. In winter, the NPF was very rare in Hyytiälä, and in 2009 and 2012 there were no winter NPF events at all.

The reason for the quite substantial variation in the event frequency between the years has

**Table 1.** Median values and trends in the parameters related to new particle formation, particle formation and growth rates. Statistically significant trends (increasing or decreasing) are shown in boldface, and 5th and 95th percentiles of the trend values are given in brackets.

| Parameter  | 1997–2012<br>median value | Relative trend (% year <sup>-1</sup> ) |                          |                          |                          |                           |
|--|---------------------------|--|--------------------------|--------------------------|--------------------------|---------------------------|
|  |                           | All data                               | Spring                   | Summer                   | Autumn                   | Winter                    |
| SO <sub>2</sub> (ppb)                                    | 0.17                      | <b>-1.6</b> [-2.2; -0.9]               | <b>-2.5</b> [-3.7; -1.3] | -0.5 [-1.6; 0.8]         | <b>-2.8</b> [-3.6; -1.8] | -0.8 [-2.4; 0.6]          |
| CS (s <sup>-1</sup> )                                    | 2.5 × 10 <sup>-3</sup>    | <b>-1.1</b> [-1.3; -0.8]               | <b>-1.1</b> [-2.0; -0.2] | <b>-0.7</b> [-1.1; -0.3] | <b>-1.5</b> [-2.1; -1.0] | -0.5 [-1.0; 0.2]          |
| UV-B (W m <sup>-2</sup> )                                | 0.24                      | <b>-2.0</b> [-2.8; -1.7]               | <b>-1.0</b> [-1.9; -0.2] | <b>-0.9</b> [-1.5; -0.1] | <b>-1.0</b> [-1.9; -0.4] | -0.3 [-0.7; 1.2]          |
| H <sub>2</sub> SO <sub>4</sub> proxy (cm <sup>-3</sup> ) | 8.1 × 10 <sup>5</sup>     | <b>-1.4</b> [-2.5; -0.6]               | <b>-2.4</b> [-3.3; -1.6] | -0.3 [-1.8; 1.3]         | <b>-2.4</b> [-4.1; -1.2] | -0.6 [-2.9; 1.1]          |
| OxOrg proxy (cm <sup>-3</sup> )                          | 6.1 × 10 <sup>7</sup>     | <b>0.9</b> [0.08; 1.1]                 | <b>1.7</b> [0.7; 2.6]    | <b>0.7</b> [0.3; 1.0]    | <b>1.5</b> [0.8; 2.2]    | -0.9 [-3.0; 1.4]          |
| T (°C)   | 4.4                       | 0.04 [-0.1; 0.1]                       | <b>0.1</b> [0.02; 0.2]   | 0.01 [-0.1; 0.1]         | 0.1 [-0.1; 0.2]          | <b>-0.2</b> [-0.4; -0.01] |
| N <sub>3-25</sub> (cm <sup>-3</sup> )                    | 220                       | <b>-1.4</b> [-2.2; -1.0]               | <b>-1.1</b> [-2.4; -0.2] | <b>-0.8</b> [-1.6; -0.1] | <b>-1.2</b> [-2.0; -0.5] | <b>-2.0</b> [-3.1; -0.9]  |
| N <sub>25-100</sub> (cm <sup>-3</sup> )                  | 790                       | <b>-0.9</b> [-1.4; -0.8]               | <b>-0.6</b> [-1.5; -0.1] | <b>-0.6</b> [-0.9; -0.1] | <b>-1.1</b> [-1.5; -0.8] | <b>-1.1</b> [-1.9; -0.5]  |
| N <sub>100-1000</sub> (cm <sup>-3</sup> )                | 370                       | <b>-1.0</b> [-1.3; -0.7]               | <b>-1.3</b> [-2.2; -0.2] | <b>-0.5</b> [-0.9; -0.1] | <b>-1.6</b> [-2.1; -1.0] | -0.3 [-0.9; 0.3]          |
| J <sub>3</sub> (cm <sup>3</sup> s <sup>-1</sup> )        | 0.84                      | 0.4 [-1.0; 1.8]                        | 1.1                      | 2.2                      | -0.5                     | -3.2                      |
| GR (nm h <sup>-1</sup> )                                 | 2.5                       | 0.5 [-0.3; 1.3]                        | 0.1                      | 1.2                      | -0.1                     | 0.9                       |

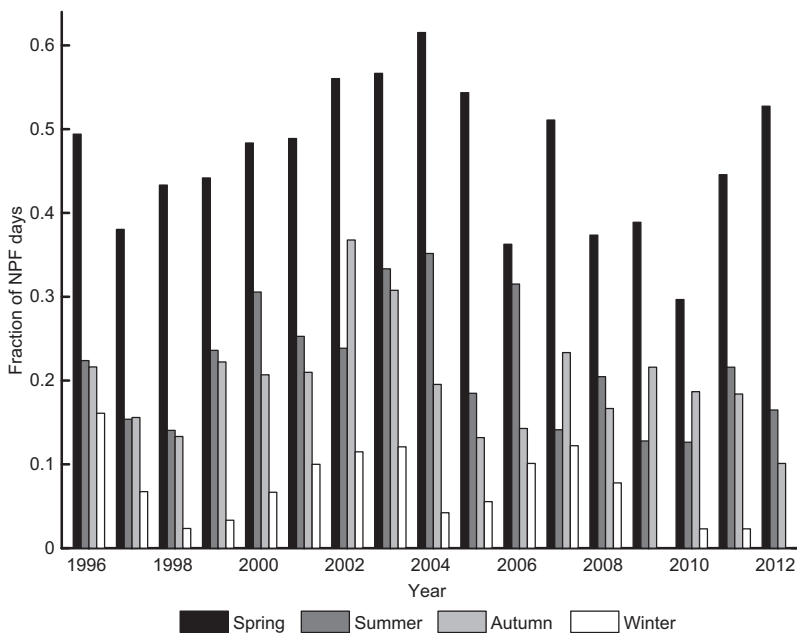


**Fig. 1.** Seasonal fractions of new particle formation (NPF) event days of all analyzed days in years 1996–2012.

not been fully explained. Kulmala *et al.* (2010) showed that the 11-year solar cycle associated with the activity of the sun is not connected to the number of NPF events in Hyytiälä. In fact, Kulmala *et al.* (2010) observed that there was a slight negative correlation between the yearly number of event days and cosmic-ray-induced atmospheric ionization intensity. This means that during those years when the ion production rate in the atmosphere was higher there were fewer NPF events. This finding suggests that ion-induced nucleation is not a dominant mechanism in atmospheric nucleation occurring in Hyytiälä, or at least the magnitude of variation in the cosmic-ray-induced ionization is not large enough to produce an observable effect in the atmospheric particle formation frequency and intensity.

The direction of the arriving air masses has been found to influence the probability of the NPF in Hyytiälä (Nilsson *et al.* 2001, Sogacheva *et al.* 2005, Dal Maso *et al.* 2007), the sector from west to north being most favorable for the NPF. We found that the yearly number of NPF event days was strongly related to the fraction of air masses that had spent their last 30 hours in the sector 260°–30° before their arrival at Hyytiälä (Fig. 2). The air coming from this direction is typically very clean, reducing the coagulation sink for newly-formed particles and condensa-

tion sink for condensing vapours. Tunved *et al.* (2006) showed that low-volatile vapours formed from the oxidation of biogenic VOCs emitted from the large boreal forest areas participate in the growth of submicron aerosol particles. Thus, the yearly variation in the arrival directions of air masses to Hyytiälä partly explains the year-to-year variation in the number of NPF days.

In summary, the probability of the NPF was at the maximum of about 40%–50% during spring (March, April and May), and a second maximum of about 30%–40% took place in September (Fig. 3). In winter, < 10% of the days were NPF event days. These findings are consistent with those by Dal Maso *et al.* (2005, 2007) who analysed the event statistics in Hyytiälä based on the first nine years of aerosol measurements at the station during the years 1996–2004. The similarity between these investigations suggests that there has not been a major change in the factors influencing the seasonality of the NPF at this measurement site.

### Connection between NPF, gas-phase sulphuric acid and organic compounds

When comparing the seasonal distribution of the fraction of NPF event days and  $[\text{H}_2\text{SO}_4]_{\text{proxy}}$



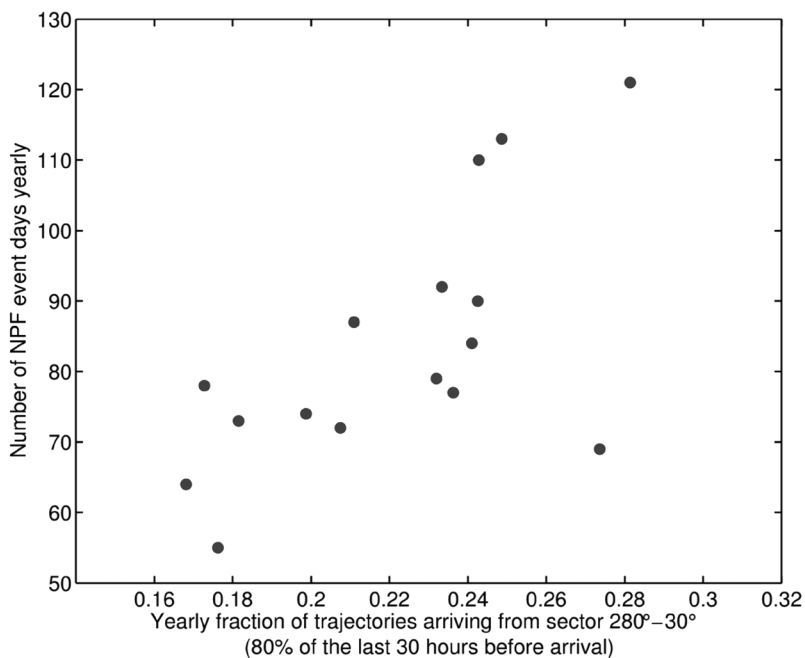


**Fig. 2.** Yearly number of NPF event days as a function of the fraction of air masses that were within the sector 280°–30° during 30 hours before arrival at Hyytiälä.

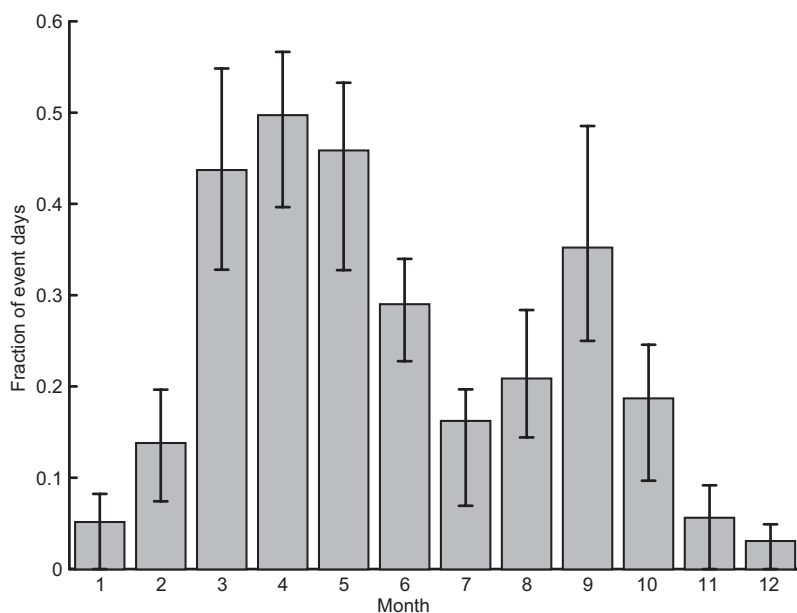


**Fig. 3.** Fraction of NPF event days of all analyzed days in each month in the years 1996–2012; error bars show the monthly minimum and maximum.

(Figs. 3 and 4), it can be seen that both had their absolute maxima during the spring months of March and April, and that  $[\text{H}_2\text{SO}_4]_{\text{proxy}}$  had another, smaller maximum in September at the same time as the NPF frequency had its maximum. The seasonal variation of  $[\text{H}_2\text{SO}_4]_{\text{proxy}}$  is

affected by the seasonal cycles of the  $\text{SO}_2$  concentration and condensation sink. The  $\text{SO}_2$  concentration had a maximum in winter (Fig. 4), starting to rise in November–December and reaching the annual maximum of about 0.5 ppb in February, and then declining to low levels

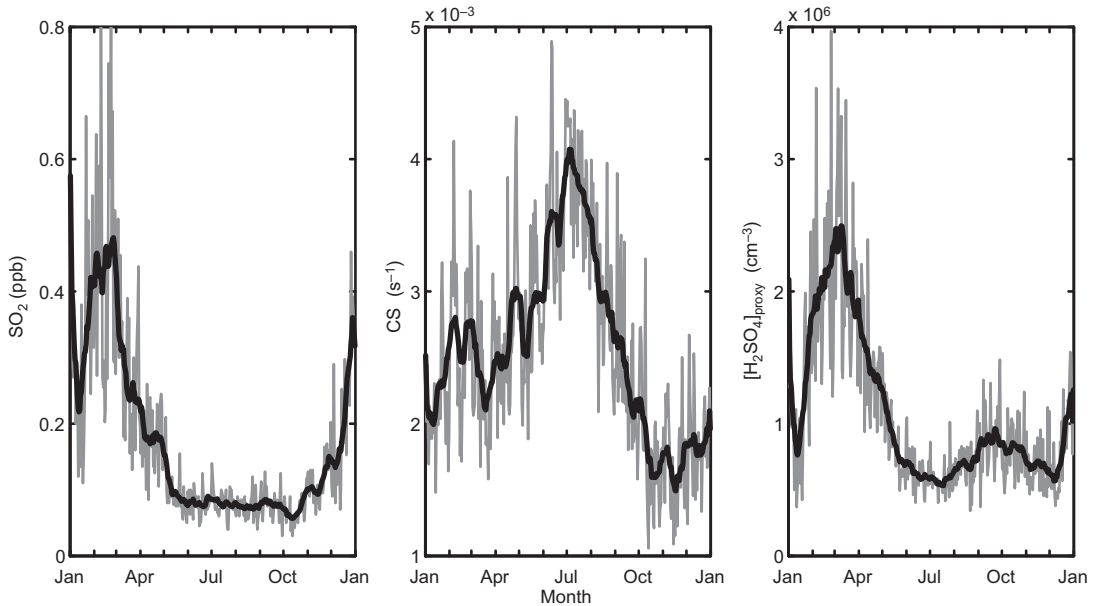


**Fig. 4.** Seasonal distributions of  $\text{SO}_2$ , condensation sink (CS) and sulphuric acid concentration evaluated by proxy ( $[\text{H}_2\text{SO}_4]_{\text{proxy}}$ ). Grey lines represents daily average values and black lines are the 30-day running mean of daily average values.

of about 0.1 ppb in May–September. The high winter  $\text{SO}_2$  concentrations are connected to increased emissions from energy and heat production during winter and also to slower atmospheric photochemistry due to the low intensity of sunlight. Also the boundary layer height is typically smaller in winter, causing the concentrations of pollutants near the ground to be higher. The condensation sink reached the highest values during summer (June–August).

We investigated the probability of particle formation as a function of  $[\text{H}_2\text{SO}_4]_{\text{proxy}}$  and  $[\text{OxOrg}]_{\text{proxy}}$ . Paasonen *et al.* (2010) showed that the nucleation rate in Hyytiälä can be related to the concentration of sulphuric acid or, even more so, to the combination of  $\text{H}_2\text{SO}_4$  and  $[\text{OxOrg}]_{\text{proxy}}$ . We constructed a nucleation parameter as the product of  $[\text{H}_2\text{SO}_4]_{\text{proxy}}$  and  $[\text{OxOrg}]_{\text{proxy}}$  (Fig. 5). It can be clearly seen that with an increasing sulphuric-acid concentration alone, as well as with the increasing product of sulphuric acid and oxidized organics concentrations, the number of NPF days increased and the number of non-NPF days decreased. However, the sulphuric-acid concentration alone did not separate the NPF days from the non-NPF days very effectively. Most of the non-NPF and also undefined days

occurred when the average daytime sulphuric acid concentration was around  $1 \times 10^6 \text{ cm}^{-3}$  and the distribution of the NPF days had its maximum at sulphuric-acid concentrations of about  $2 \times 10^6 \text{ cm}^{-3}$ . On the other hand, the maxima of the NPF and non-NPF days were separated by one order of magnitude in the daytime values of the product of  $[\text{H}_2\text{SO}_4]_{\text{proxy}}$  and  $[\text{OxOrg}]_{\text{proxy}}$ . When this nucleation parameter increased to values larger than  $2 \times 10^{14} \text{ cm}^{-6}$ , more than half of the days were NPF event days, and less than 10% of the days had no new-particle formation. The distribution of the undefined days first increased, then started to decrease and remained at about 20% at the highest values of the nucleation parameter. It might be argued that the undefined days are somewhat “failed” NPF events (particle concentrations low, growth of the particles not continuous, newly formed particles not observed starting from the smallest sizes), and that this type of the NPF starts to take place already at lower values of the nucleation parameter. In fact, Buenrostro Mazon *et al.* (2009) identified many of the undefined days in Hyytiälä to have ambient conditions resembling more those of the NPF days than non-NPF days. Many of these undefined days were found in summer when the

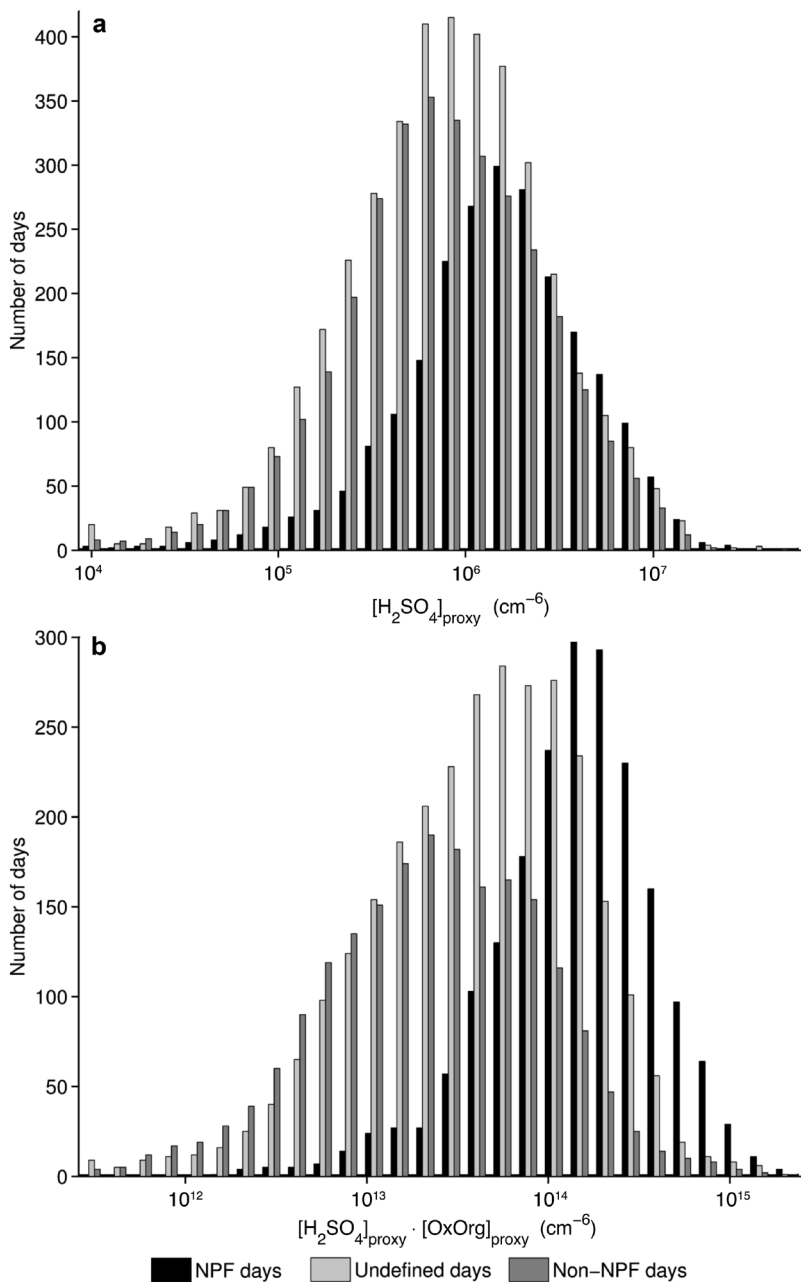


**Fig. 5.** (a) The number of nucleation event (NPF), non-event (Non-NPF) and undefined days as a function of  $[H_2SO_4]_{4proxy}$ , and (b) the product of  $[H_2SO_4]_{4proxy}$  and  $[OxOrg]_{proxy}$ . Each bin represents the average daytime value (between 09:00 and 15:00) of the nucleation parameter.

concentrations of oxidized organics are the highest annual levels.

The exponent of the power-law dependence between the new-particle formation rate and gaseous sulphuric acid concentration has traditionally been used to get information about the nucleation mechanism (Kulmala *et al.* 2006, Sihto *et al.* 2006, Riipinen *et al.* 2007). It should

be kept in mind, however, that the smallest particles observed in this study had a diameter of 3 nm, whereas nucleation itself is expected to take place at sizes of around 1.5 nm (Kulmala *et al.* 2013a). As a result, the value of the exponent might have been affected by particle losses during their growth from 1.5 to 3 nm (e.g. Ehrhart and Curtius 2013), changes in the particle growth

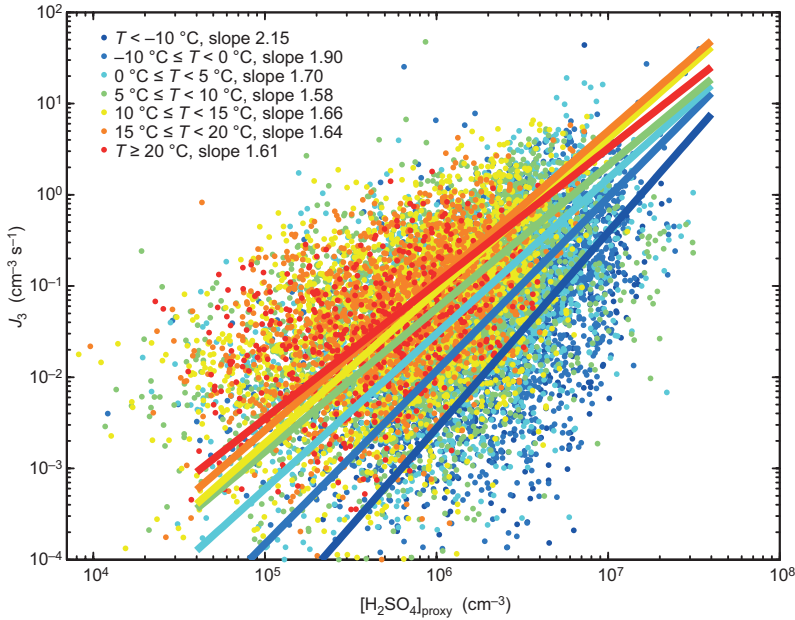


**Fig. 6.** Formation rate of 3-nm particles,  $J_3$ , as a function of  $[\text{H}_2\text{SO}_4]_{\text{proxy}}$  within different temperatures ranges. The lines show linear fits made to the data within the indicated temperature ranges. Each data point corresponds to 30-min averaged data during the NPF events.

rate below 3 nm (e.g. Sihto *et al.* 2009, Korhonen *et al.* 2014), or the potential presence of stable pre-critical clusters below 3 nm (Vehkamäki *et al.* 2012). In our measurement data set, the exponent of the power-law dependence between  $J_3$  and  $[\text{H}_2\text{SO}_4]_{\text{proxy}}$  appeared to vary between 1 and 2 depending on atmospheric conditions (Fig. 6). If we look at the data more carefully and group it according to the ambient temperature, we may see that the exponent was close to (or even higher than) 2 at the coldest temperatures below  $-10\text{ °C}$  and decreased to about 1.6 as the temperature was above  $20\text{ °C}$ . This indicates that at higher temperatures, vapors other than sulphuric acid — very likely low-volatile organic vapours (see also Kulmala *et al.* 1998) — have a larger role in the initial steps of new-particle formation and growth.

The correlation coefficient between  $J_3$  and  $[\text{H}_2\text{SO}_4]_{\text{proxy}}$  in the entire data set was 0.55. This correlation decreased with an increasing temperature: for the data points below  $-10\text{ °C}$  it was 0.61, while for the data measured at the temperatures above  $20\text{ °C}$  it was 0.37. Correlating the particle formation rate with the product of  $[\text{H}_2\text{SO}_4]_{\text{proxy}}$  and  $[\text{OxOrg}]_{\text{proxy}}$  for the whole data set resulted in about the same correlation coefficient as was obtained between the particle formation rate and sulphuric acid concentration alone.

This is consistent with the results of Paasonen *et al.* (2010) who also did not find a better correlation when including the oxidized organics. The correlation coefficient between the particle formation rate and the product of  $[\text{H}_2\text{SO}_4]_{\text{proxy}}$  and  $[\text{OxOrg}]_{\text{proxy}}$  increased with increasing temperatures, being 0.41 for the data below  $-10\text{ °C}$  and 0.51 for the data above  $20\text{ °C}$ .

At any constant  $[\text{H}_2\text{SO}_4]_{\text{proxy}}$ , the observed formation rate of 3-nm particles varied by up to 3 orders of magnitude between the lowest and highest temperatures (Fig. 6). This is consistent with the observations by Sihto *et al.* (2006) and Riipinen *et al.* (2007), who found that the nucleation coefficients varied more than one order of magnitude during spring measurements in Hyytiälä. The temperature dependence of the formation rate is very likely related, at least to some extent, to changes in the emissions of biogenic volatile organic compounds (BVOC). The highest ambient temperatures were observed in summer when BVOC emissions are at their highest. Atmospheric oxidation of BVOCs produces low-volatile vapours which contribute to both nucleation and new-particle growth (Kulmala *et al.* 2013a).

Compared with the particles formation rate, the particle growth rate may be even more sensitive to quantities other than the sulphuric acid

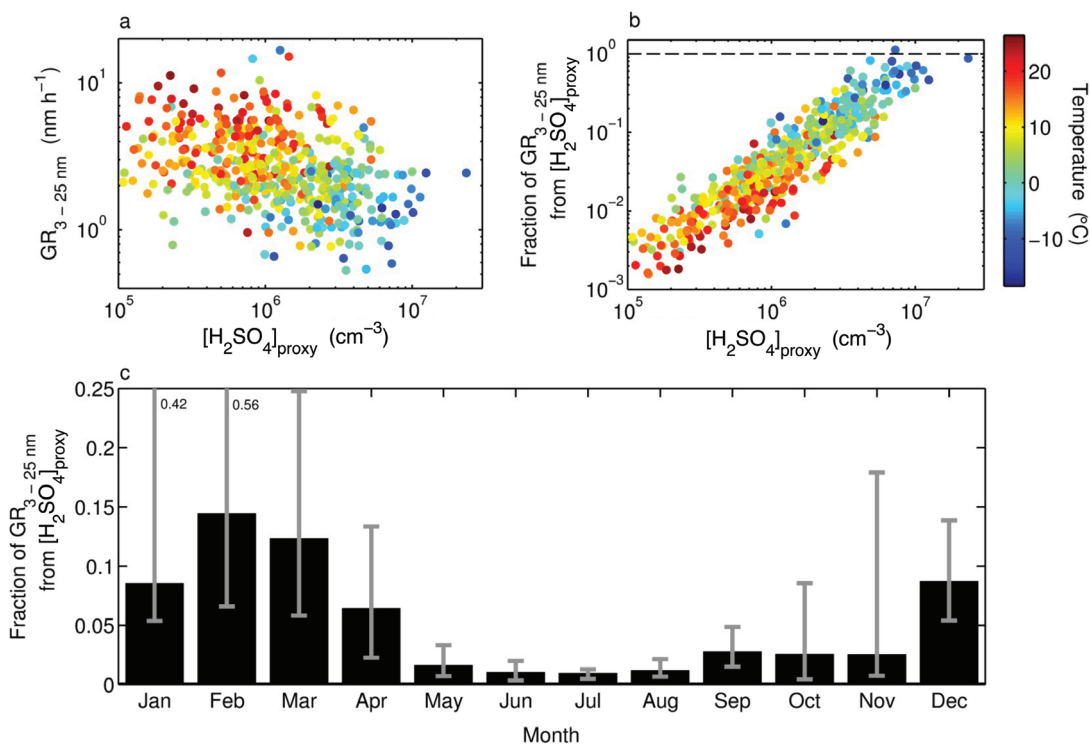


**Fig. 7.** (a) Nucleation mode (3–25 nm particles) growth rates as a function of  $[\text{H}_2\text{SO}_4]_{\text{proxy}}$ , and (b) the fraction of growth rate explained by sulphuric acid condensation as a function of  $[\text{H}_2\text{SO}_4]_{\text{proxy}}$ . (c) Monthly medians of the growth rate explained by sulphuric acid; error bars show 25th and 75th percentiles (upper percentiles for January and February are indicated next to the error bars).

concentration. In our data set, there was an overall tendency of having lower particle growth rates at higher  $[\text{H}_2\text{SO}_4]_{\text{proxy}}$ , even though the data were quite scattered (Fig. 7a). The fraction of the particle growth rate that was estimated to be caused by  $\text{H}_2\text{SO}_4$  condensation (calculated by Eq. 3) is clearly related to  $[\text{H}_2\text{SO}_4]_{\text{proxy}}$  (see Fig. 7b). This fraction was the highest in winter and early spring and lowest in summertime (Fig. 7c). In February and March, more than 10% of the growth was on average due to  $\text{H}_2\text{SO}_4$ . This is consistent with the results of Boy *et al.* (2005) who studied the contribution of  $\text{H}_2\text{SO}_4$  to the growth rate of nucleation mode particles in Hyttälä using modelled  $\text{H}_2\text{SO}_4$  concentrations for March–April 2003, and estimated that on average 3%–17% of the particle growth could be explained by condensation of  $\text{H}_2\text{SO}_4$ . From May to August, the contribution of  $\text{H}_2\text{SO}_4$  to the particle growth was only a few percent. When taking into account the temperature, nucleation mode

particle growth rates were found to increase with increasing temperatures (Fig. 7b). However, even in the lowest temperatures there were only a few NPF events during which all the observed particle growth could be explained by  $\text{H}_2\text{SO}_4$  condensation. This further supports the importance of BVOC oxidation products in the NPF and growth observed in Hyttälä.

Finally, we investigated the relation between the nucleation mode particle concentration,  $N_{3-25}$ , and their formation and growth rate (Fig. 8). The value of  $N_{3-25}$  tended to increase with increasing values of  $J_3$  during all seasons, as one would expect. On the contrary,  $N_{3-25}$  did not correlate with the particle growth rate, except during summer when a moderate negative correlation between these two quantities existed. This latter feature can be explained by a shorter lifetime of nucleation mode particles due to their more rapid growth out of the mode during summer. The particle formation and growth rates appeared to



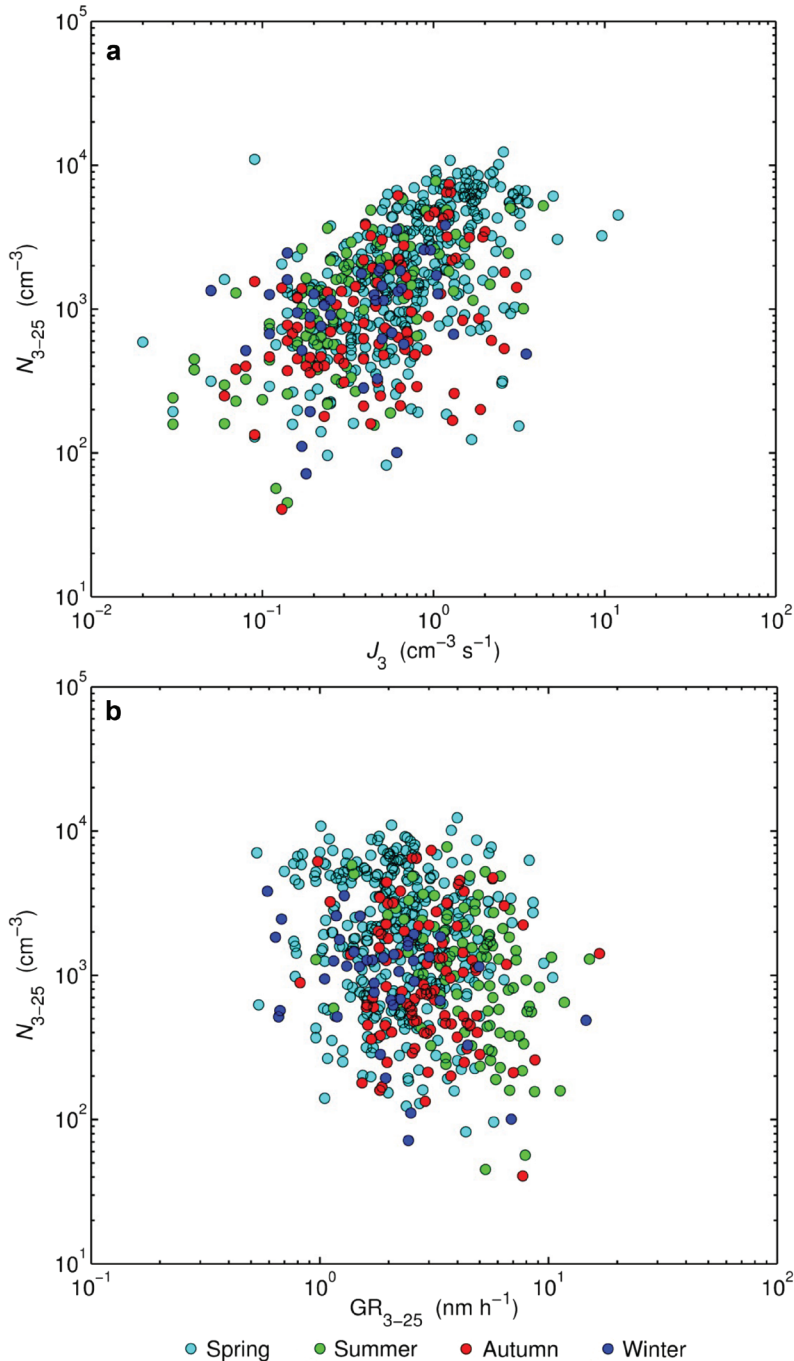


**Fig. 8.** Nucleation mode particle concentrations as a function of (a) the particle formation rate, and (b) growth rate. Each data point corresponds to the median during the NPF event. Seasons are indicated by the color of the data points.

have no correlation with each other, indicating that the vapors participating in the initial steps of new-particle formation were, at least partly, different from those contributing to the later growth of the particles.

### Variability and long-term trend in particle number concentrations

The nucleation mode particle number concentration had a decreasing trend over the whole time

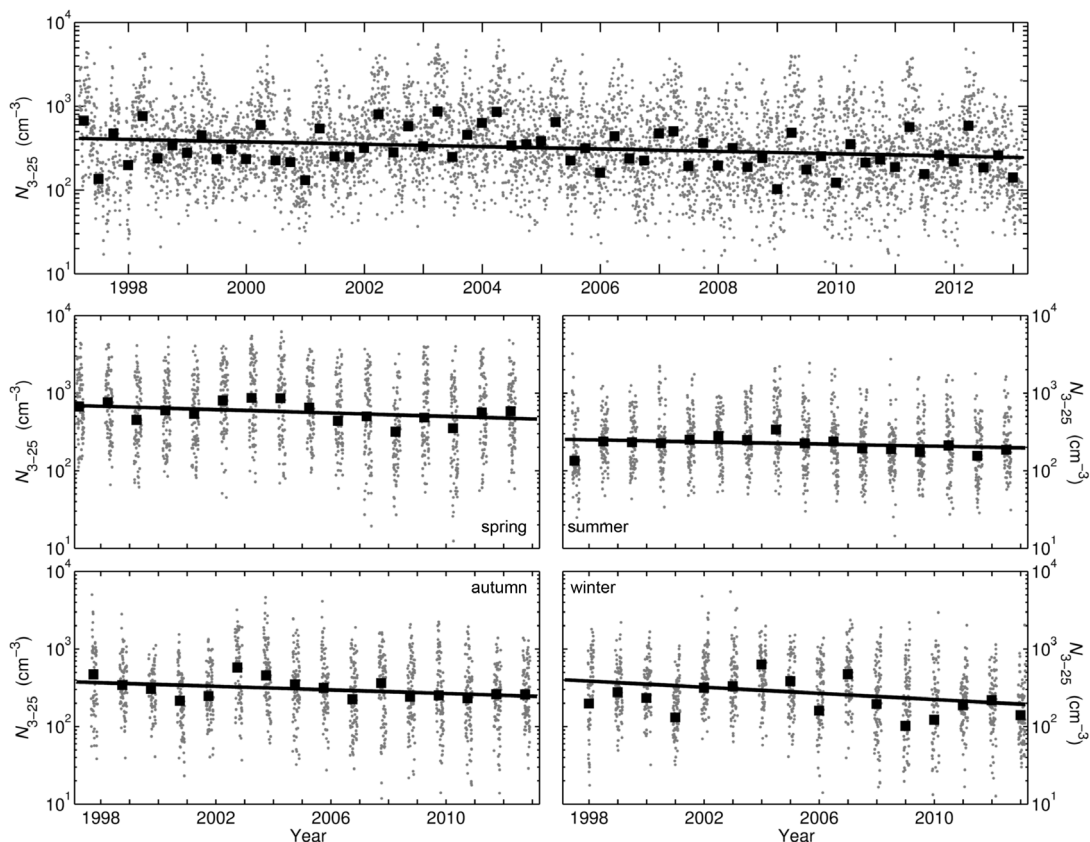


**Fig. 9.** Nucleation mode particle number concentrations in the whole time series (1997–2012, top panel), and seasonally (lower panels). Grey points are daily averages and black squares show seasonal medians. Black lines show the linear trends fitted to the daily values.

series and in all seasons (Fig. 9 and Table 1). Similar decreasing trends were found in the data divided between the clean and outside-the-clean sector, or between NPF and non-NPF days,

(Table 2), even though the trend was not statistically significant for the clean sector. The outside-the-clean sector Aitken mode (25–100 nm) particle number concentrations were decreasing

**Table 2.** Trends calculated separately for days when air masses arrive from the clean sector (280°–30°) and from outside the sector, as well as for NPF days and non-NPF days. Statistically significant trends (increasing or decreasing) are shown in boldface, and 5th and 95th percentiles of the trend values are given in brackets.

| Parameter                            | Relative trend (% year <sup>-1</sup> ) |                          |                          |                          |
|--------------------------------------|--|--------------------------|--------------------------|--------------------------|
|                                      | Clean sector                           | Outside clean sector     | NPF days                 | Non-NPF days             |
| SO <sub>2</sub>                      | <b>-1.2</b> [-2.0; -0.6]               | <b>-1.4</b> [-2.2; -0.8] | <b>-2.6</b> [-3.9; -1.7] | <b>-1.7</b> [-2.7; -1.0] |
| CS                                   | <b>-0.7</b> [-1.2; -0.3]               | <b>-1.1</b> [-1.4; -0.8] | <b>-1.1</b> [-1.8; -0.4] | <b>-1.2</b> [-1.3; -0.9] |
| UV-B                                 | -1.3 [-4.5; 4.2]                       | -0.9 [-2.1; 0.06]        | -0.3 [-1.4; 0.5]         | 0.06 [-3.1; 0.5]         |
| H <sub>2</sub> SO <sub>4</sub> proxy | <b>-0.9</b> [-1.8; -0.4]               | -0.6 [-1.7; 0.1]         | <b>-1.3</b> [-2.1; -0.8] | -0.3 [-1.4; 0.6]         |
| N <sub>3-25</sub>                    | <b>-0.7</b> [-1.6; 0.04]               | <b>-1.7</b> [-2.4; -1.3] | <b>-0.9</b> [-1.7; -0.3] | <b>-0.9</b> [-1.9; -0.4] |
| N <sub>25-100</sub>                  | -0.04 [-1.0; 0.06]                     | <b>-1.1</b> [-1.5; -0.8] | <b>-0.8</b> [-1.3; -0.3] | <b>-0.8</b> [-1.2; -0.6] |
| N <sub>100-1000</sub>                | <b>-0.9</b> [-1.6; -0.3]               | <b>-1.2</b> [-1.6; -1.0] | <b>-1.3</b> [-2.1; -0.5] | <b>-1.0</b> [-1.2; -0.8] |

as well. In the accumulation mode, a decreasing trend was seen regardless of the sector chosen, which is consistent with the decreasing trends at several European stations found by Asmi *et al.* (2013). These decreasing trends of particle number concentrations suggest a major role of decreasing anthropogenic emissions in the S–SE sector (i.e. in air masses arriving at Hyytiälä from central and eastern Europe), emphasizing the important contribution of long-range transported anthropogenic pollutants to observed particle number concentrations.

### Sulphuric acid and its precursors

The SO<sub>2</sub> concentration decreased in Hyytiälä from the annual average of 0.24 ppb in 1997 to around 0.12 ppb in 2012 (Fig. 10a). The median SO<sub>2</sub> concentration during the whole observation period was 0.17 ppb, which is low as compared with that at many locations in central Europe (Vestreng *et al.* 2007). The overall trend of the SO<sub>2</sub> concentration in Hyytiälä was  $-1.6\%$  year<sup>-1</sup> with some seasonal variability (Table 1). Similar decreasing trends have been found also at other measurement sites in Finland, the main reason being the measures taken to improve air quality (Anttila *et al.* 2010). The highest SO<sub>2</sub> concentrations in Hyytiälä were recorded during winter, typically in January and February, reaching values above 1 ppb also in the latest years of the study period. The strongest decrease in the SO<sub>2</sub> concentration occurred in spring and autumn (almost  $-3\%$  year<sup>-1</sup>). Similar to SO<sub>2</sub>, the condensation sink was decreasing in Hyytiälä at a rate of  $-1.1\%$  year<sup>-1</sup> (Fig. 10b), except in winter when the decrease was not statistically significant. The value of condensation sink is determined mainly by accumulation mode particles, so any changes in primary particle emissions such as those from energy production, industry and traffic, or changes in aerosol precursor emissions combined with atmospheric ageing, also influence CS. Compared with Hyytiälä, larger decreases in both SO<sub>2</sub> concentration and CS were observed in Värriö, Finnish Lapland, where the concentrations had been higher and governed by emissions from the Russian industry activities (Kyrö *et al.* 2014).

The amount of UV-B radiation decreased in Hyytiälä with an overall trend of  $-2.0\%$  year<sup>-1</sup> (Fig. 10c). This decrease was recorded for all the seasons except winter, and was also apparent in the other measured quantities related to solar radiation, such as global radiation and photosynthetically-active radiation. One possible explanation for this decrease is an increase in cloudiness. We examined the monthly mean total cloud cover data from the ECMWF global atmospheric reanalysis (ERA-INTERIM, Dee *et al.* 2011). We found an increasing trend of  $0.7\%$  year<sup>-1</sup> for the cloud cover in the area around Hyytiälä. Similar increasing trends in cloudiness over Scandinavia have been reported by Eastman and Warren (2013) based on a longer time-series analysis of cloud observations.

$[\text{H}_2\text{SO}_4]_{\text{proxy}}$  is equal to the ratio of its source and sink terms when assuming a steady state. The main source is the oxidation of sulphur dioxide by OH radicals in the atmosphere, and the sink is defined by condensation onto pre-existing particle surfaces. H<sub>2</sub>SO<sub>4</sub> is typically assumed to have a very low vapor pressure and it sticks to all surfaces it comes into contact. While both the sink and the source terms of sulphuric acid have a decreasing trend in Hyytiälä, the trend in SO<sub>2</sub> and hence in the source term is slightly stronger ( $-1.6\%$  year<sup>-1</sup> for SO<sub>2</sub> and  $-1.1\%$  year<sup>-1</sup> for CS). This together with the decreasing level of radiation, causes an overall decreasing trend in  $[\text{H}_2\text{SO}_4]_{\text{proxy}}$ . Corresponding to the high winter SO<sub>2</sub> concentrations in 2011, the 2011 winter values of  $[\text{H}_2\text{SO}_4]_{\text{proxy}}$  were the highest during the 16-year period. This did not, however, affect the overall trend, and it did not result in the higher-than-usual NPF-event probability in the winter of 2011. During winter, the NPF is probably limited by the availability of sunlight and organic compounds.

Decreasing trends in SO<sub>2</sub> and CS were found also when examining the data separately for the clean and outside-the-clean sector, as well as for both NPF and non-NPF days (Table 2). However, in case of  $[\text{H}_2\text{SO}_4]_{\text{proxy}}$  a statistically significant decreasing trend was found only for the days when air masses arrived from the clean sector, or for the NPF days.

$[\text{H}_2\text{SO}_4]_{\text{proxy}}$  had a very strong, seasonal variation in Hyytiälä. The highest concentrations were

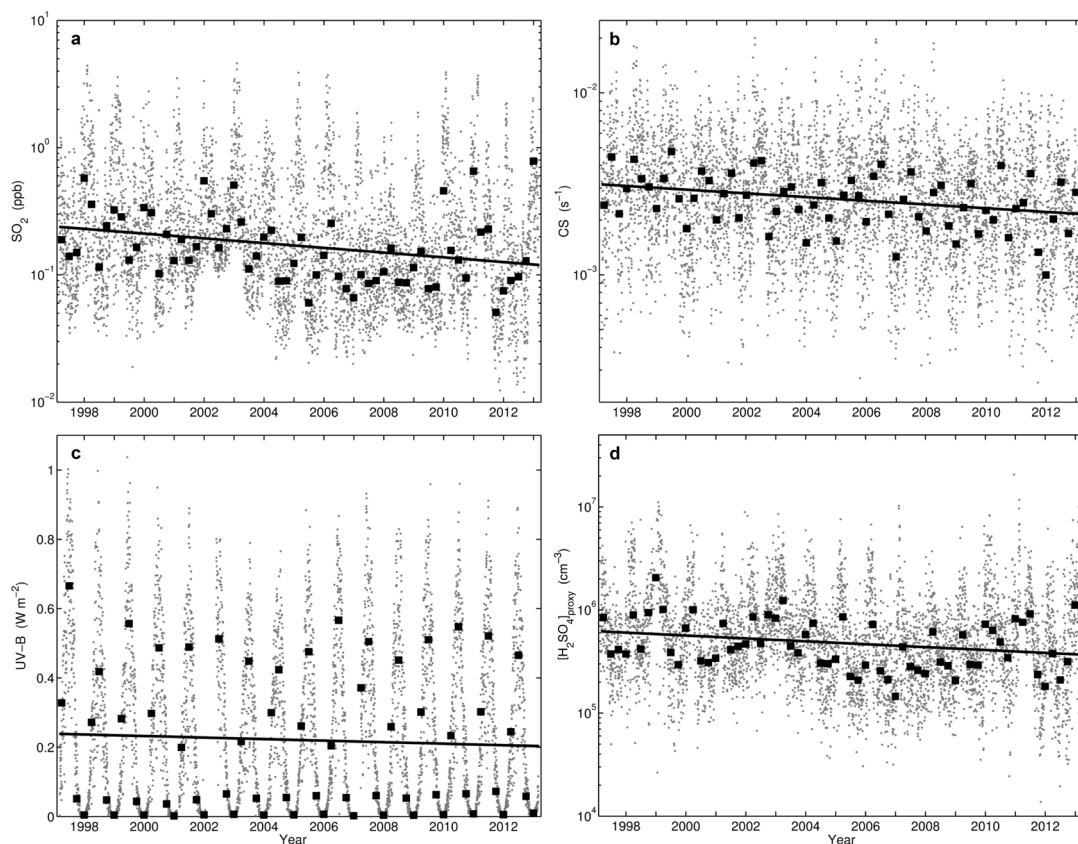


**Fig. 10.** (a)  $\text{SO}_2$  concentration, (b) condensation sink, (c) UV-B radiation intensity, and (d)  $[\text{H}_2\text{SO}_4]_{4\text{proxy}}$  time series over the period 1997–2012. Grey points are daily averages, black squares are seasonal averages, and linear trends for each variable are shown with the black solid lines.

found for winter (January–February) and they decrease towards summer. This is similar to the seasonal variation in  $[\text{H}_2\text{SO}_4]_{4\text{proxy}}$  in Värriö (Kyrö *et al.* 2014), but different from that reported for Pallas, another Finnish Lapland site, that had no clear seasonal pattern (Asmi *et al.* 2011a). Apparently, this calls for further studies as other long-term data sets will become available.

### New-particle formation and growth

Both formation and growth rates of nucleation mode particles were increasing at an overall trend of 0.2%–0.5%  $\text{year}^{-1}$  (Fig. 11 and Table 1), however the trends were not statistically significant according to the confidence interval criteria. New-particle formation and growth rates seem to have increased most during summer, which

is also the season with the smallest decreasing trend in  $[\text{H}_2\text{SO}_4]_{4\text{proxy}}$  (Table 1).

The overall year-to-year variation in the intensity of NPF events peaked in 2002–2004 (Fig. 11). This is the same time as the yearly number of NPF event days had its maximum, indicating that the NPF-initiating processes and contributing to the overall intensity of particle formation both depend on the ambient  $\text{H}_2\text{SO}_4$  concentration. Significant decreasing trends in the concentration of  $\text{SO}_2$ , a precursor vapour for  $\text{H}_2\text{SO}_4$ , and the condensation sink, i.e. the loss term of sulphuric acid, during the 16-year observation period were found. The amount of UV-B radiation responsible for the atmospheric OH radical production decreased during the observation period, even though there were also differences among the years in the annual average UV-B radiation (Fig. 10c). The decrease in  $\text{SO}_2$

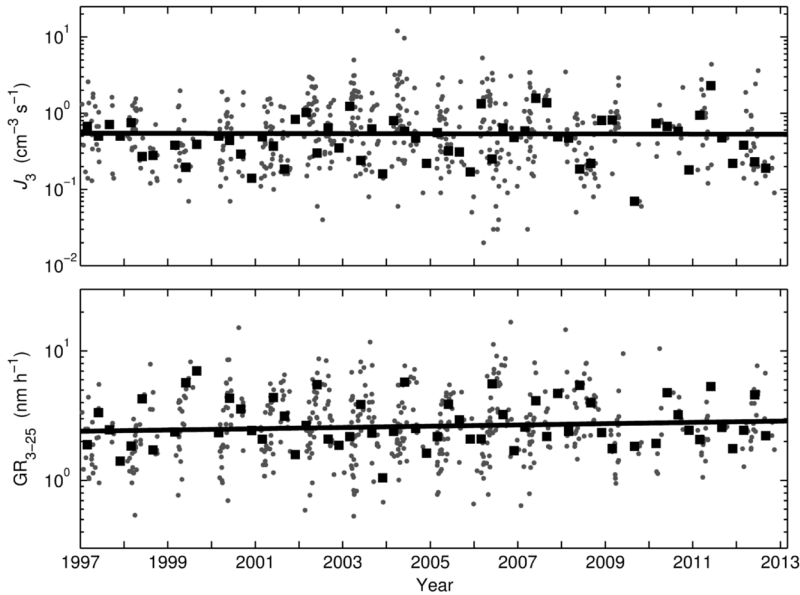


**Fig. 11.** Formation and growth rates of 3–25 nm nucleation mode particles. Grey points show values determined for individual NPF events and black squares seasonal medians. Linear trends are shown with black solid lines.

concentrations is connected to overall air quality improvements observed all over Europe (e.g. Denby *et al.* 2010), and is considered to be one of the prime reasons for the global decrease in the particle number concentrations (Asmi *et al.* 2013). The condensation sink and in general the particulate matter concentrations also follow the air quality improvements, as was found in studies on air pollutants in Finland by Anttila *et al.* (2010). The more rapid decrease rate of the  $\text{SO}_2$  concentration as compared with that of the particulate matter concentration explains the overall decreasing trend in  $[\text{H}_2\text{SO}_4]_{\text{proxy}}$ , especially during the NPF days when the  $\text{SO}_2$  decrease was twice as rapid as compared with that in CS, which has resulted in larger decreases in  $[\text{H}_2\text{SO}_4]_{\text{proxy}}$  on the NPF days as compared with that on the non-NPF days (Table 2).

In contrast to the trends in the nucleation mode particle formation and growth rates, the concentrations of nucleation mode particles in Hyttiälä were decreasing, as evidenced by the trend in the whole time series and by the seasonal trends (Fig. 9). A decrease in the nucleation mode particle concentrations was also found in the study by Riuttanen *et al.* (2013) who examined the nucleation mode concentrations during the years 1996–2008 based the air mass origin, and found that the concentrations were decreasing in both clean and polluted air masses arriving at

Hyttiälä. The decrease rate was greater in those air masses that came from south-east and were thus influenced more by anthropogenic pollution as compared with other air masses. This suggests that the NPF in the Hyttiälä boreal forest environment is determined by the processes inhibiting formation, such as the magnitude of the coagulation sink by pre-existing particles, rather than by the processes enabling formation. The observed decreasing particulate matter concentrations might suggest that the magnitude of the NPF in Hyttiälä will increase in the future. This, together with the decreasing coagulation sink, would enable a larger fraction of the newly formed particles to grow to the sizes at which they can act as cloud condensation nuclei, i.e. larger than about 50–100 nm in diameter (Kerminen *et al.* 2012).

The emissions of biogenic VOCs depend on the ambient temperature. In Hyttiälä there seems to be a small but not statistically significant increase in temperature (Table 1). Seasonally, the highest increase of  $0.1\% \text{ year}^{-1}$  was recorded for spring while in winter there was a decrease of  $-0.2\% \text{ year}^{-1}$ . Both these trends were statistically significant. During summer and autumn the average temperatures increased less and the trends were not statistically significant. When examining  $[\text{OxOrg}]_{\text{proxy}}$ , we found statistically significant and increasing trends for spring, summer and autumn, and a decreasing trend for winter.



$[\text{H}_2\text{SO}_4]_{\text{proxy}}$  decreased in spring and autumn but not in summer (the trend not significant statistically). Both these findings, i.e. increase in concentrations of oxidized organics and no decrease in sulphuric acid concentrations, can be linked to the increasing nucleation mode particle formation ( $2.2\% \text{ year}^{-1}$ ) and growth ( $1.2\% \text{ year}^{-1}$ ) rates in summer. The trends in the formation and growth rates were, however, not statistically significant due to the large variability in the measured values. One explanation for such variability could be the opposite concentration trends in sulphuric acid and oxidized organics.

Another factor affecting emissions of biogenic VOC is the increasing atmospheric  $\text{CO}_2$  concentration, which increases photosynthesis and gross primary production (GPP) of the forest. Kulmala *et al.* (2013b) found that in Hyytiälä, the particle growth rate due to condensation of oxidized organic compounds in March–August correlated positively with the GPP of the forest in the conditions where the ambient temperature was in the range of  $18\text{--}23\text{ }^\circ\text{C}$ . The increase in this growth rate was about  $7\%$  over the period 1996–2011, which is comparable to the summer relative trend of  $1.2\% \text{ year}^{-1}$  in the growth rate of nucleation mode particles found in our study. Thus, both the increasing concentrations of oxidized organics and  $\text{CO}_2$  are likely to enhance the particle growth rates in the future.

## Summary and conclusions

We analyzed the trends in particle formation probabilities, formation and growth rates, and their connections to  $[\text{H}_2\text{SO}_4]_{\text{proxy}}$  and  $[\text{OxOrg}]_{\text{proxy}}$  based on 16-year data set from a boreal forest environment. A notable year-to-year variation in the number of NPF days was found. This variation was found to be linked to the annual frequency of air masses originating from the Atlantic and Arctic oceans arriving to Hyytiälä from the W–NE sector. The pattern of seasonal variation in the NPF remained the same as compared with that reported in the earlier studies carried out at the same site, and is linked to the seasonal cycle of  $[\text{H}_2\text{SO}_4]_{\text{proxy}}$ .

The probability of the NPF could be described better by the product of  $[\text{H}_2\text{SO}_4]_{\text{proxy}}$

and  $[\text{OxOrg}]_{\text{proxy}}$  than by  $[\text{H}_2\text{SO}_4]_{\text{proxy}}$  alone. The relation between the particle formation rate and  $[\text{H}_2\text{SO}_4]_{\text{proxy}}$  was found to depend on the ambient temperature, suggesting that oxidized organics originating from biogenic emissions play an important role in the new-particle formation. The overall correlations between the particle formation rate and either  $[\text{H}_2\text{SO}_4]_{\text{proxy}}$  or the product of  $[\text{H}_2\text{SO}_4]_{\text{proxy}}$  and  $[\text{OxOrg}]_{\text{proxy}}$  were similar. The contribution of  $\text{H}_2\text{SO}_4$  to particle growth rates was found to be minor. In winter, the fraction of growth explained by  $[\text{H}_2\text{SO}_4]_{\text{proxy}}$  was typically on the order of  $10\%$ , and in summer it decreased to a few percent.

The  $\text{SO}_2$  concentration and condensation sink decreased during our measurement period, as did also the particle number concentrations in the nucleation, Aitken and accumulation modes. Such decreases were seen also when separating the data based on the air mass source area, or when looking at separately the NPF and non-NPF days. The trends in the particle formation and growth rates were smaller than that in the nucleation mode particle concentration and they were also more variable between the seasons.  $[\text{OxOrg}]_{\text{proxy}}$  had an increasing trend in all the seasons except winter. Since both sulphuric acid and oxidized organics are known to influence new-particle formation (Kulmala *et al.* 2013a), their different trends might partly explain the non-significant trends in the particle formation and growth rates.

*Acknowledgements:* This research was supported by the Academy of Finland Center of Excellence program (grant no. 1118615). The ERA-INTERIM re-analysis data were obtained from the European Centre for Medium-range Weather Forecasts (ECMWF). The NOAA Air Research Laboratory (ARL) is acknowledged for the provision of the HYSPLIT transport model and READY website.

## References

- Aalto P., Hämeri K., Becker E., Weber R., Salm J., Mäkelä J.M., Hoell C., O'Dowd C.D., Karlsson H., Hansson H.-C., Väkevä M., Koponen I.K., Buzorius G. & Kulmala M. 2001. Physical characterization of aerosol particles during nucleation events. *Tellus* 53B: 344–358.
- Ahlm L., Julin J., Fountoukis C., Pandis S.N. & Riipinen I. 2013. Particle number concentrations over Europe in 2030: the role of emissions and new particle formation. *Atmos. Chem. Phys.* 13: 10271–10283.

- Almeida J., Schobesberger S., Kürten A., Ortega I.K., Kupiainen-Määttä O., Praplan A., Adamov A., Amorim A., Bianchi F., Breitenlechner M., David A., Dommen J., Donahue N.M., Downard A., Dunne E., Duplissy J., Ehrhart S., Flagan R.C., Franchin A., Guida R., Hakala J., Hansel A., Heinritzi M., Henschel H., Jokinen T., Junninen H., Kajos M., Kangasluoma J., Keskinen H., Kupc A., Kurtén T., Kvashin A.N., Laaksonen A., Lehtipalo K., Leiminger M., Leppä J., Loukonen V., Makhmutov V., Mathot S., McGrath M.J., Nieminen T., Olenius T., Onnela A., Petäjä T., Riccobono F., Riipinen I., Rissanen M., Rondo L., Ruuskanen T., Santos F.D., Sarnela N., Schallhart S., Schnitzhofer R., Seinfeld J.H., Simon M., Sipilä M., Stozhkov Y., Stratmann F., Tomé A., Tröstl J., Tsagkogeorgas G., Vaattovaara P., Viisanen Y., Virtanen A., Vrtala A., Wagner P.E., Weingartner E., Wex H., Williamson C., Wimmer D., Ye P., Yli-Juuti T., Carslaw K.S., Kulmala M., Curtius J., Baltensperger U., Worsnop D.R., Vehkamäki H. & Kirkey J. 2013. Molecular understanding of sulphuric acid–amine particle nucleation in the atmosphere. *Nature* 502: 359–363.
- Anttila P. & Tuovinen J.-P. 2010. Trends of primary and secondary pollutant concentrations in Finland in 1994–2007. *Atmos. Environ.* 44: 30–41.
- Asmi E., Kivekäs N., Kerminen V.-M., Komppula M., Hyvärinen A.-P., Hatakka J., Viisanen Y. & Lihavainen H. 2011a. Secondary new particle formation in northern Finland Pallas site between the years 2000 and 2010. *Atmos. Chem. Phys.* 11: 12959–12972.
- Asmi A., Collaud Coen M., Ogren J.A., Andrews E., Sheridan P., Jefferson A., Weingartner E., Baltensperger U., Bukowiecki N., Lihavainen H., Kivekäs N., Asmi E., Aalto P.P., Kulmala M., Wiedensohler A., Birmili W., Hamed A., O'Dowd C., Jennings S.G., Weller R., Flentje H., Fjaeraa A.M., Fiebig M., Myhre C.L., Hallar A.G., Swietlicki E., Kristensson A. & Laj P. 2013. Aerosol decadal trends — Part 2: *in-situ* aerosol particle number concentrations at GAW and ACTRIS stations. *Atmos. Chem. Phys.* 13: 895–916.
- Asmi A., Wiedensohler A., Laj P., Fjaeraa A.-M., Sellegri K., Birmili W., Weingartner E., Baltensperger U., Zdimal V., Zikova N., Putaud J.-P., Marinoni A., Tunved P., Hansson H.-C., Fiebig M., Kivekäs N., Lihavainen H., Asmi E., Ulevicius V., Aalto P.P., Swietlicki E., Kristensson A., Mihalopoulos N., Kalivitis N., Kalapov I., Kiss G., de Leeuw G., Henzing B., Harrison R.M., Beddows D., O'Dowd C., Jennings S.G., Flentje H., Weinhold K., Meinhardt F., Ries L. & Kulmala M. 2011b. Number size distributions and seasonality of submicron particles in Europe 2008–2009. *Atmos. Chem. Phys.* 11: 5505–5538.
- Birmili W., Berresheim H., Plass-Dülmer C., Elste T., Gilge S., Wiedensohler A. & Uhrner U. 2003. The Hohenpeisenberg aerosol formation experiment (HAFEX): a long-term study including size-resolved aerosol, H<sub>2</sub>SO<sub>4</sub>, OH, and monoterpenes measurements. *Atmos. Chem. Phys.* 3: 361–376.
- Boy M., Kulmala M., Ruuskanen T.M., Pihlatie M., Reisel A., Aalto P.P., Keronen P., Dal Maso M., Hellen H., Hakola H., Jansson R., Hanke M. & Arnold F. 2005. Sulphuric acid closure and contribution to nucleation mode particle growth. *Atmos. Chem. Phys.* 5: 863–878.
- Boy M., Mogensen D., Smolander S., Zhou L., Nieminen T., Paasonen P., Plass-Dülmer C., Sipilä M., Petäjä T., Mauldin L., Berresheim H. & Kulmala M. 2013. Oxidation of SO<sub>2</sub> by stabilized Criegee intermediate (sCI) radicals as a crucial source for atmospheric sulfuric acid concentrations. *Atmos. Chem. Phys.* 13: 3865–3879.
- Buenrostro Mazon S., Riipinen I., Schultz D.M., Valtanen M., Dal Maso M., Sogacheva L., Junninen H., Nieminen T., Kerminen V.-M. & Kulmala M. 2009. Classifying previously undefined days from eleven years of aerosol-particle-size distribution data from the SMEAR II station, Hyttiälä, Finland. *Atmos. Chem. Phys.* 9: 667–676.
- Collaud Coen M., Andrews E., Asmi A., Baltensperger U., Bukowiecki N., Day D., Fiebig M., Fjaeraa A.M., Flentje H., Hyvärinen A., Jefferson A., Jennings S.G., Kouvarakis G., Lihavainen H., Lund Myhre C., Malm W.C., Mihapopoulos N., Molenaar J.V., O'Dowd C., Ogren J.A., Schichtel B.A., Sheridan P., Virkkula A., Weingartner E., Weller R. & Laj P. 2013. Aerosol decadal trends — Part 1: *in-situ* optical measurements at GAW and IMPROVE stations. *Atmos. Chem. Phys.* 13: 869–894.
- Dal Maso M., Kulmala M., Riipinen I., Wagner R., Hussein T., Aalto P.P. & Lehtinen K.E.J. 2005. Formation and growth of fresh atmospheric aerosols: eight years of aerosol size distribution data from SMEAR II, Hyttiälä, Finland. *Boreal Env. Res.* 10: 323–336.
- Dal Maso M., Sogacheva L., Aalto P.P., Riipinen I., Komppula M., Tunved P., Korhonen L., Suur-Uski V., Hirsikko A., Kurtén T., Kerminen V.-M., Lihavainen H., Viisanen Y., Hansson H.-C. & Kulmala M. 2007. Aerosol size distribution measurements at four Nordic field stations: identification, analysis and trajectory analysis of new particle formation bursts. *Tellus* 59B: 350–361.
- Dee D.P., Uppala S.M., Simmons A.J., Berrisford P., Poli P., Kobayashi S., Andrae U., Balmaseda M.A., Balsamo G., Bauer P., Bechtold P., Beljaars A.C.M., van de Berg L., Bidlot J., Bormann N., Delsol C., Dragani R., Fuentes M., Geer A.J., Haimberger L., Healy S.B., Hersbach H., Hólm E.-V., Isaksen I., Kållberg P., Köhler M., Matricardi M., McNally A.P., Monge-Sanz B.M., Morcrette J.-J., Park B.-K., Peubey C., de Rosnay P., Tavolato C., Thépaut J.-N. & Vitart F. 2011. The ERA-Interim reanalysis: configuration and performance of the data assimilation system. *Quat. J. R. Meteorol. Soc.* 137: 553–597.
- Denby B., Sundvor I., Cassiani M., de Smet P., de Leeuw G. & Horálek J. 2010. Spatial mapping of ozone and SO<sub>2</sub> trends in Europe. *Sci. Total Environ.* 408: 4795–4806.
- Eastman R. & Warren S.G. 2013. A 39-yr survey of cloud changes from land stations worldwide 1971–2009: long-term trends, relation to aerosols, and expansion of the tropical belt. *J. Climate* 26: 1286–1303.
- Ehn M., Vuollekoski H., Petäjä T., Kerminen V.-M., Vana M., Aalto P., de Leeuw G., Ceburnis D., Dupuy R., O'Dowd C.D. & Kulmala M. 2010. Growth rates during coastal and marine new particle formation in western Ireland. *J. Geophys. Res.* 115, D18218, doi:10.1029/2010JD014292.

- Ehrhart S. & Curtius J. 2013. Influence of aerosol lifetime on the interpretation of nucleation experiments with respect to the first nucleation theorem. *Atmos. Chem. Phys.* 13: 11465–11471.
- Ghan S.J., Smith S.J., Wang M., Zhang K., Pringle K.J., Carslaw K.S., Pierce J.R., Bauer S.E. & Adams P.J. 2013. A simple model of global aerosol indirect effects. *J. Geophys. Res.* 118: 6688–6707.
- Hari P. & Kulmala M. 2005. Station for Measuring Ecosystem–Atmosphere Relations (SMEAR II). *Boreal Env. Res.* 10: 315–322.
- Hess A., Iyer H. & Malm W. 2001. Linear trend analysis: a comparison of methods. *Atmos. Environ.* 35: 5211–5222.
- Hirsikko A., Laakso L., Hörrak U., Aalto P.P., Kerminen V.-M. & Kulmala M. 2005. Annual and size dependent variation of growth rates and ion concentrations in boreal forest. *Boreal Env. Res.* 10: 357–369.
- Hussein T., Dal Maso M., Petäjä T., Koponen I.K., Paatero P., Aalto P.P., Hämeri K. & Kulmala M. 2005. Evaluation of an automatic algorithm for fitting the particle number size distributions. *Boreal Env. Res.* 10: 337–355.
- IPCC 2013. *Climate change 2013: the physical science basis*. Working Group I Contribution to the Fifth Assessment Report of the Intergovernmental Panel on Climate Change, Cambridge University Press, Cambridge, United Kingdom and New York, NY, USA.
- Junninen H., Hulkkonen M., Riipinen I., Nieminen T., Hirsikko A., Suni T., Boy M., Lee S.-H., Vana M., Tammet H., Kerminen V.-M. & Kulmala M. 2008. Observations on nocturnal growth of atmospheric clusters. *Tellus* 60B: 365–371.
- Kalivitis N., Stavroulas I., Bougiatioti A., Kouvarakis G., Gagné S., Manninen H.E., Kulmala M. & Mihalopoulos N. 2012. Night-time enhanced atmospheric ion concentrations in the marine boundary layer. *Atmos. Chem. Phys.* 12: 3627–3638.
- Kerminen V.-M., Lihavainen H., Komppula M., Viisanen Y. & Kulmala M. 2005. Direct observational evidence linking atmospheric aerosol formation and cloud droplet activation. *Geophys. Res. Lett.* 32, L14803, doi:10.1029/2005GL023130.
- Kerminen V.-M., Petäjä T., Manninen H.E., Paasonen P., Nieminen T., Sipilä M., Junninen H., Ehn M., Gagne S., Laakso L., Riipinen I., Vehkamäki H., Kurtén T., Ortega I.K., Dal Maso M., Brus D., Hyvärinen A., Lihavainen H., Leppä J., Lehtinen K.E.J., Mirme A., Mirme S., Hörrak U., Berndt T., Stratmann F., Birmili W., Wiedensohler A., Metzger A., Dönnen J., Baltensperger U., Kiendler-Scharr A., Mentel T.F., Wildt J., Winkler P.M., Wagner P.E., Petzold A., Minikin A., Plass-Dülmer C., Pöschl U., Laaksonen A. & Kulmala M. 2010. Atmospheric nucleation: highlights of the EUCAARI project and future directions. *Atmos. Chem. Phys.* 10: 10829–10848.
- Kerminen V.-M., Paramonov M., Anttila T., Riipinen I., Fountoukis C., Korhonen H., Asmi E., Laakso L., Lihavainen H., Swietlicki E., Svenningsson B., Asmi A., Pandis S.N., Kulmala M. & Petäjä T. 2012. Cloud condensation nuclei production associated with atmospheric nucleation: a synthesis based on existing literature and new results. *Atmos. Chem. Phys.* 12: 12037–12059.
- Kirkby J., Curtius J., Almeida J., Dunne E., Duplissy J., Ehrhart S., Franchin A., Gagné S., Ickes L., Kürten A., Kupc A., Metzger A., Riccobono F., Rondo L., Schobesberger S., Tsagkogeorgas G., Wimmer D., Amorim A., Bianchi F., Breitenlechner M., David A., Dommer J., Downard A., Ehn M., Flagan R., Haider S., Hansel A., Hauser D., Jud W., Junninen H., Kreissl F., Kvashin A., Laaksonen A., Lehtipalo K., Lima J., Lovejoy E.R., Makhmutov V., Mathot S., Mikkilä J., Minginette P., Mogo S., Nieminen T., Onnela A., Pereira P., Petäjä T., Schnitzhofer R., Seinfeld J.H., Sipilä M., Stozhkov Y., Stratmann F., Tomé A., Vanhanen J., Viisanen Y., Vrtala A., Wagner P.E., Walther H., Weingartner E., Wex H., Winkler P.M., Carslaw K.S., Worsnop D.R., Baltensperger U. & Kulmala M. 2010. Role of sulphuric acid, ammonia and galactic cosmic rays in atmospheric aerosol nucleation. *Nature* 476: 429–433.
- Korhonen H., Kerminen V.-M., Kokkola H. & Lehtinen K.E.J. 2014. Estimating atmospheric nucleation rates from size distribution measurements: Analytical equations for the case of size dependent growth rates. *J. Aerosol Sci.* 69: 13–20.
- Korhonen P., Kulmala M., Laaksonen A., Viisanen Y., McGraw R. & Seinfeld J.H. 1999. Ternary nucleation of H<sub>2</sub>SO<sub>4</sub>, NH<sub>3</sub> and H<sub>2</sub>O in the atmosphere. *J. Geophys. Res.* 104: 26349–26353.
- Krejci R., Ström J., Reus M., Hoor P., Williams J., Fischer H. & Hansson H.-C. 2003. Evolution of aerosol properties over the rain forest in Surinam, South America, observed from aircraft during the LBA-CLAIRE 98 experiment. *J. Geophys. Res.* 108, 4561, doi:10.1029/2001JD001375.
- Kulmala M. & Kerminen V.-M. 2008. On the formation and growth of atmospheric nanoparticles. *Atmos. Res.* 90: 132–150.
- Kulmala M., Lehtinen K.E.J. & Laaksonen A. 2006. Cluster activation theory as an explanation of the linear dependence between formation rate of 3 nm particles and sulphuric acid concentration. *Atmos. Chem. Phys.* 6: 787–793.
- Kulmala M., Toivonen A., Mäkelä M. & Laaksonen A. 1998. Analysis of the growth of nucleation mode particles observed in boreal forest. *Tellus* 50B: 449–462.
- Kulmala M., Korhonen P., Napari I., Karlsson A., Berresheim H. & O’Dowd C.D. 2003. Aerosol formation during PARFORCE: Ternary nucleation of H<sub>2</sub>SO<sub>4</sub>, NH<sub>3</sub> and H<sub>2</sub>O. *J. Geophys. Res.* 107(D19), 8111, doi: 10.1029/2001JD000900.
- Kulmala M., Vehkamäki H., Petäjä T., Dal Maso M., Lauri A., Kerminen V.-M., Birmili W. & McMurry P.H. 2004. Formation and growth rates of ultrafine atmospheric particles: a review of observations. *J. Aerosol Sci.* 35: 143–176.
- Kulmala M., Petäjä T., Nieminen T., Sipilä M., Manninen H.E., Lehtipalo K., Dal Maso M., Aalto P.P., Junninen H., Paasonen P., Riipinen I., Lehtinen K.E.J., Laaksonen A. & Kerminen V.-M. 2012. Measurement of the nucleation of atmospheric aerosol particles. *Nature Protoc.* 7: 1651–1667.
- Kulmala M., Riipinen I., Nieminen T., Hulkkonen M.,

- Sogacheva L., Manninen H.E., Paasonen P., Petäjä T., Dal Maso M., Aalto P.P., Viljanen A., Usoskin I., Vainio R., Mirme S., Mirme A., Minikin A., Petzold A., Hörrak U., Plass-Dülmer C., Birmili W. & Kerminen V.-M. 2010. Atmospheric data over a solar cycle: no connection between galactic cosmic rays and new particle formation. *Atmos. Chem. Phys.* 10: 1885–1898.
- Kulmala M., Kontkanen J., Junninen H., Lehtipalo K., Manninen H.E., Nieminen T., Petäjä T., Sipilä M., Schobesberger S., Rantala P., Franchin A., Jokinen T., Järvinen E., Äijälä M., Kangasluoma J., Hakala J., Aalto P.P., Paasonen P., Mikkilä J., Vanhanen J., Aalto J., Hakola H., Makkonen U., Ruuskanen T., Mauldin R.L.III, Duplissy J., Vehkamäki H., Bäck J., Kortelainen A., Riipinen I., Kurtén T., Johnston M.V., Smith J.N., Ehn M., Mentel T.F., Lehtinen K.E.J., Laaksonen A., Kerminen V.-M. & Worsnop D.R. 2013a. Direct observation of atmospheric aerosol nucleation. *Science* 339: 943–946.
- Kulmala M., Nieminen T., Nikandrova A., Lehtipalo K., Manninen H.E., Kajos M.K., Kolari P., Lauri A., Petäjä T., Krejci R., Hansson H.-C., Swietlicki E., Lindroth A., Christensen T.R., Arneth A., Hari P., Bäck J., Vesala T. & Kerminen V.-M. 2014. CO<sub>2</sub>-induced terrestrial climate feedback mechanism: From carbon sink to aerosol source and back. *Boreal Env. Res.* 19 (suppl. B): 122–131.
- Kurtén T., Loukonen V., Vehkamäki H. & Kulmala M. 2008. Amines are likely to enhance neutral and ion-induced sulfuric acid-water nucleation in the atmosphere more effectively than ammonia. *Atmos. Chem. Phys.* 8: 4095–4103.
- Kyrö E.-M., Väänänen R., Kerminen V.-M., Virkkula A., Petäjä T., Asmi A., Dal Maso M., Nieminen T., Juhola S., Shcherbinin A., Riipinen I., Lehtipalo K., Keronen P., Aalto P.P., Hari P. & Kulmala M. 2013. Trends in new particle formation in Eastern Lapland, Finland: effect of decreasing sulphur emissions from Kola Peninsula. *Atmos. Chem. Phys.* 14: 4383–4396.
- Laakso L., Merikanto J., Vakkari V., Laakso H., Kulmala M., Molefe M., Kgabi N., Mabaso D., Carslaw K.S., Spracklen D.V., Lee L.A., Reddington C.L. & Kerminen V.-M. 2013. Boundary layer nucleation as a source of new CCN in savannah environment. *Atmos. Chem. Phys.* 13: 1957–1972.
- Laaksonen A., Hamed A., Joutsensaari J., Hiltunen L., Cavalli F., Junkermann W., Asmi A., Fuzzi S. & Facchini M.C. 2005. Cloud condensation nuclei production from nucleation events at a highly polluted region. *Geophys. Res. Lett.* 32, 06812, doi:10.1029/2004GL022092.
- Lappalainen H.K., Sevanto S., Bäck J., Ruuskanen T.M., Kolari P., Taipale R., Rinne J., Kulmala M. & Hari P. 2009. Day-time concentrations of biogenic volatile organic compounds in a boreal forest canopy and their relation to environmental and biological factors. *Atmos. Chem. Phys.* 9: 5447–5459.
- Lee L.A., Pringle K.J., Reddington C.L., Mann G.W., Stier P., Spracklen D.V., Pierce J.R. & Carslaw K.S. 2013. The magnitude and causes of uncertainty in global model simulations of cloud condensation nuclei. *Atmos. Chem. Phys.* 13: 8879–8914.
- Loukonen V., Kurtén T., Ortega I.K., Vehkamäki H., Pádúa A.A.H., Sellegri K. & Kulmala M. 2010. Enhancing effect of dimethylamine in sulfuric acid nucleation in the presence of water — a computational study. *Atmos. Chem. Phys.* 10: 4961–4974.
- Makkonen R., Asmi A., Kerminen V.-M., Boy M., Arneth A., Hari P. & Kulmala M. 2012. Air pollution control and decreasing new particle formation lead to strong climate warming. *Atmos. Chem. Phys.* 12: 1515–1524.
- Mauldin R.L.III, Berndt T., Sipilä M., Paasonen P., Petäjä T., Kim S., Kurtén T., Stratmann F., Kerminen V.-M. & Kulmala M. 2012. A new atmospherically relevant oxidant of sulphur dioxide. *Nature* 488: 193–196.
- Merikanto J., Spracklen D.V., Mann G.W., Pickering S.J. & Carslaw K.S. 2009. Impact of nucleation on global CCN. *Atmos. Chem. Phys.* 9: 8601–8616.
- Metzger A., Verheggen B., Dommen J., Duplissy J., Prevot A.S.H., Weingartner E., Riipinen I., Kulmala M., Spracklen D.V., Carslaw K. & Baltensperger U. 2010. Evidence for the role of organics in aerosol particle formation under atmospheric conditions. *Proc. Natl. Acad. Sci. USA* 107: 6646–6651.
- Mikkonen S., Romakkaniemi S., Smith J.N., Korhonen H., Petäjä T., Plass-Duelmer C., Boy M., McMurry P.H., Lehtinen K.E.J., Joutsensaari J., Hamed A., Mauldin R.L.III, Birmili W., Spindler G., Arnold F., Kulmala M. & Laaksonen A. 2011. A statistical proxy for sulphuric acid concentration. *Atmos. Chem. Phys.* 11: 11319–11334.
- Mudelsee, M. 2010. *Climate time series analysis*. Springer, Heidelberg.
- Mäkelä J.M., Aalto P., Jokinen V., Pohja T., Nissinen A., Palmroth S., Markkanen T., Seitsonen K., Lihavainen H. & Kulmala M. 1997. Observations of ultrafine aerosol particle formation and growth in boreal forest. *Geophys. Res. Lett.* 24: 1219–1222.
- Nieminen T., Lehtinen K.E.J. & Kulmala M. 2010. Sub-10 nm particle growth by vapor condensation — effects of vapor molecule size and particle thermal speed. *Atmos. Chem. Phys.* 10: 9773–9779.
- Nieminen T., Manninen H.E., Sihto S.-L., Yli-Juuti T., Mauldin R.L.III, Petäjä T., Riipinen I., Kerminen V.-M. & Kulmala M. 2009. Connection of sulfuric acid to atmospheric nucleation in boreal forest. *Environ. Sci. Technol.* 43: 4715–4721.
- O’Dowd C., Jimenez J., Bahreini R., Flagan R., Seinfeld J., Hämeri K., Pirjola L., Kulmala M., Jennings S. & Hoffmann T. 2002. Marine aerosol formation from biogenic iodine emissions. *Nature* 417: 632–636.
- Paasonen P., Nieminen T., Asmi E., Manninen H.E., Petäjä T., Plass-Dülmer C., Flentje H., Birmili W., Wiedensohler A., Hörrak U., Metzger A., Hamed A., Laaksonen A., Facchini M.C., Kerminen V.-M. & Kulmala M. 2010. On the roles of sulphuric acid and low-volatility organic vapours in the initial steps of atmospheric new particle formation 2010. *Atmos. Chem. Phys.* 10: 11223–11242.
- Paasonen P., Asmi A., Petäjä T., Kajos M.K., Äijälä M., Junninen H., Holst T., Abbatt J.P.D., Arneth A., Birmili W., Denier van der Gon H., Hamed A., Hoffer A., Laakso L., Laaksonen A., Leitch W.R., Plass-Dülmer



- C., Pryor S.C., Räisänen P., Swietlicki E., Wiedensohler A., Worsnop D.R., Kerminen V.-M. & Kulmala M. 2013. Warming-induced increase in aerosol number concentration likely to moderate climate change. *Nature Geosci.* 6: 438–442.
- Paramonov M., Aalto P.P., Asmi A., Prisle N., Kerminen V.-M., Kulmala M. & Petäjä T. 2013. The analysis of size-segregated cloud condensation nuclei counter (CCNC) data and its implications for aerosol-cloud interactions. *Atmos. Chem. Phys.* 13: 10285–10301.
- Petäjä T., Mauldin R.L.III, Kosciuch E., McGrath J., Nieminen T., Paasonen P., Boy M., Adamov A., Kotiaho T. & Kulmala M. 2009. Sulfuric acid and OH concentrations in a boreal forest site. *Atmos. Chem. Phys.* 9: 7435–7448.
- Petäjä T., Sipilä M., Paasonen P., Nieminen T., Kurtén T., Ortega I.K., Stratmann F., Vehkamäki H., Berndt T. & Kulmala M. 2011. Experimental observation of strongly bound dimers of sulfuric acid: application to nucleation in the atmosphere. *Phys. Rev. Lett.* 106, 228302, doi:10.1103/PhysRevLett.106.228302.
- Riipinen I., Sihto S.-L., Kulmala M., Arnold F., Dal Maso M., Birmili W., Saarnio K., Teinilä K., Kerminen V.-M., Laaksonen A. & Lehtinen K.E.J. 2007. Connections between atmospheric sulphuric acid and new particle formation during QUEST III–IV campaigns in Heidelberg and Hyytiälä. *Atmos. Chem. Phys.* 7: 1899–1914.
- Riuttanen L., Hulkkonen M., Dal Maso M., Junninen & Kulmala M. 2013. Trajectory analysis of atmospheric transport of fine particles, SO<sub>2</sub>, NO<sub>x</sub> and O<sub>3</sub> to the SMEAR II station in Finland in 1996–2008. *Atmos. Chem. Phys.* 13: 2153–2164.
- Rohrer F. & Berresheim H. 2006. Strong correlation between levels of tropospheric hydroxyl radicals and solar ultraviolet radiation. *Nature* 442: 184–187.
- Sihto S.-L., Kulmala M., Kerminen V.-M., Dal Maso M., Petäjä T., Riipinen I., Korhonen H., Arnold F., Janson R., Boy M., Laaksonen A. & Lehtinen K.E.J. 2006. Atmospheric sulphuric acid and aerosol formation: implications from atmospheric measurements for nucleation and early growth mechanisms. *Atmos. Chem. Phys.* 6: 4079–4091.
- Sihto S.-L., Vuollekoski H., Leppä J., Riipinen I., Kerminen V.-M., Korhonen H., Lehtinen K.E.J., Boy M. & Kulmala M. 2009. Aerosol dynamics simulations on the connection of sulphuric acid and new particle formation. *Atmos. Chem. Phys.* 9: 2933–2947.
- Sihto S.-L., Mikkilä J., Vanhanen J., Ehn M., Liao L., Lehtipalo K., Aalto P.P., Duplissy J., Petäjä T., Kerminen V.-M., Boy M. & Kulmala M. 2011. Seasonal variation of CCN concentrations and aerosol activation properties in boreal forest. *Atmos. Chem. Phys.* 11: 13269–13285.
- Sipilä M., Berndt T., Petäjä T., Brus D., Vanhanen J., Stratmann F., Patokoski J., Mauldin R.L.III, Hyvärinen A.-P., Lihavainen H. & Kulmala M. 2010. The role of sulfuric acid in atmospheric nucleation. *Science* 327: 1243–1246.
- Sogacheva L., Dal Maso M., Kerminen V.-M. & Kulmala M. 2005. Probability of nucleation events and aerosol particle concentrations in different air mass types arriving at Hyytiälä, southern Finland, based on back trajectories analysis. *Boreal Env. Res.* 10: 479–491.
- Spracklen D.V., Carslaw K.S., Kulmala M., Kerminen V.-M., Sihto S.-L., Riipinen I., Merikanto J., Mann G.W., Chipperfield M.P., Wiedensohler A., Birmili W. & Lihavainen H. 2008. Contribution of particle formation to global condensation nuclei concentrations. *Geophys. Res. Lett.* 35, L06808, doi:10.1029/2007GL033038.
- Spracklen D.V. & Rap A. 2013. Natural aerosol-climate feedbacks suppressed by anthropogenic aerosol. *Geophys. Res. Lett.* 40: 5316–5319.
- Street J.O., Carroll R.J. & Ruppert D. 1998. A note on computing robust regression estimates via iteratively reweighted least squares. *The American Statistician* 42: 152–154.
- Weatherhead E.C., Reinsel G.C., Tiao G.C., Meng X.-L., Choi D., Cheang W.-K., Keller T., DeLuisi J., Wuebbles D.J., Kerr J.B., Miller A.J., Oltmans S.J. & Frederick J.E. 1998. Factors affecting the detection of trends: statistical considerations and applications to environmental data. *J. Geophys. Res.* 103: 17149–17161.
- Vehkamäki H., McGrath M.J., Kurtén T., Julin J., Lehtinen K.E.J. & Kulmala M. 2012. Rethinking the application of the first nucleation theorem to particle formation. *J. Chem. Phys.* 136, 094107, doi:10.1063/1.3689227.
- Vestreng V., Myhre G., Fagerli H., Reis S. & Tarrason L. 2007. Twenty-five years of continuous sulphur dioxide emission reduction in Europe. *Atmos. Chem. Phys.* 7: 3663–3681.
- Weber R.J., McMurry P.H., Eisele F.L. & Tanner D.J. 1995. Measurement of expected nucleation precursor species and 3 to 500 nm diameter particles at Mauna Loa Observatory, Hawaii. *J. Atmos. Sci.* 52: 2242–2257.
- Weber R.J., Lee S., Chen G., Wang B., Kapustin V., Moore K., Clarke A.D., Mauldin L., Kosciuch E., Cantrell C., Eisele F., Thornton D.C., Bandy A.R., Sachse G.W. & Fuelberg H.E. 2003. New particle formation in anthropogenic plumes advecting from Asia observed during TRACE-P. *J. Geophys. Res.* 108, 8814, doi:10.1029/2002JD003112.
- Wiedensohler A., Chen Y.F., Nowak A., Wehner B., Achtert P., Berghof M., Birmili W., Wu Z.J., Hu M., Zhu T., Takegawa N., Kita K., Kondo Y., Lou S.R., Hofzumahaus A., Holland F., Wahner A., Gunthe S.S, Rose D., Su H. & Pöschl U. 2009. Rapid aerosol particle growth and increase of cloud condensation nucleus activity by secondary aerosol formation and condensation: a case study for regional air pollution in northeastern China. *J. Geophys. Res.* 114, 00G08, doi:10.1029/2008JD010884.
- Yli-Juuti T., Nieminen T., Hirsikko A., Aalto P.P., Asmi E., Hörrak U., Manninen H.E., Patokoski J., Dal Maso M., Petäjä T., Rinne J., Kulmala M. & Riipinen I. 2011. Growth rates of nucleation mode particles in Hyytiälä during 2003–2009: variation with particle size, season, data analysis method and ambient conditions. *Atmos. Chem. Phys.* 11: 12865–12886.
- Yoon Y.J., O’Dowd C.D., Jennings S.G. & Lee S.H. 2006. Statistical characteristics and predictability of particle formation events in Mace Head. *J. Geophys. Res.* 111, D13204, doi:10.1029/2005JD006284.
- Yu F. & Luo G. 2009. Simulation of particle size distribution with a global aerosol model: contribution of nucleation



- to aerosol and CCN number concentrations. *Atmos. Chem. Phys.* 9: 7691–7710.
- Yu H., McGraw R. & Lee S.H. 2012. Effects of amines on formation of sub-3 nm particles and their subsequent growth. *Geophys. Res. Lett.* 39, L02807, doi:10.1029/2011GL050099.
- Zhao J., Smith J.N., Eisele F.L., Chen M., Kuang C. & McMurry P.H. 2011. Observation of neutral sulfuric acid-amine containing clusters in laboratory and ambient measurements. *Atmos. Chem. Phys.* 11: 10823–10836.